

# Densities and Thermal Expansion of Some Aqueous Rare Earth Chloride Solutions Between 5° and 80° C. I. LaCl<sub>3</sub>, PrCl<sub>3</sub>, and NdCl<sub>3</sub>

Wayne M. Gildseth,<sup>1</sup> Anton Habenschuss, and Frank H. Spedding<sup>2</sup>

Ames Laboratory-ERDA and Department of Chemistry, Iowa State University, Ames, Iowa 50010

A dilatometric method is used to measure densities of aqueous LaCl<sub>3</sub>, PrCl<sub>3</sub>, and NdCl<sub>3</sub> solutions from approximately 0.1 to 3.5 molal, and from 20° to 80° C for LaCl<sub>3</sub> and 5° to 80° C for PrCl<sub>3</sub> and NdCl<sub>3</sub>, at 5° intervals. Equations representing the apparent molal volumes as a function of temperature and concentration are given. Partial molal volumes, coefficients of thermal expansion, and apparent and partial molal expansibilities calculated from these fits are discussed in terms of ion-ion and ion-solvent interactions, as well as in terms of solvent structure. Water appears to undergo greater electrostriction with decreasing rare earth ionic radii, resulting in decreasing apparent and partial molal volumes at all temperatures. However, the apparent and partial molal expansibilities increase with decreasing rare earth ionic radii. The existence of an inversion temperature below which the solution is more expansible than pure water and above which the reverse is true is verified.

Investigations in this laboratory, including the determination of partial molal volumes (43, 46, 49, 50), heats of dilution (42), partial molal heat capacities (44), viscosities (45, 51-53), and electrical conductances (40, 47, 48) of aqueous rare earth solutions, have indicated that the thermodynamic and transport properties of these solutions are not simple functions of the ionic radii. It has been suggested (46) that changes in primary hydration coordination of the rare earth ions are partially responsible for the observed irregularities. Although little thermal expansion data exist for aqueous solutions containing trivalent cations (28), other recent studies (7, 8, 10, 11, 14, 27, 33-38) indicate that thermal expansion data may help elucidate the extent to which ion-ion and ion-solvent interactions, as well as solvent structure, are important in solutions.

In this investigation, densities of aqueous lanthanum, praseodymium, and neodymium chloride solutions have been measured at a number of concentrations and temperatures. Various thermodynamic properties derivable from these data have been calculated and examined in terms of types of interactions and structures which might be present in the solutions.

## Experimental

**Apparatus and procedure.** The apparatus and procedure used for the determination of the densities of water (22) were also used in this work. Two sets of dilatometers were employed: one set of nine dilatometers, Series I, was used to measure densities of LaCl<sub>3</sub> and NdCl<sub>3</sub> solutions between 20° and 80° C; and some years later, a second set of 10 dilatometers, Series II, was used to measure densities of NdCl<sub>3</sub> and PrCl<sub>3</sub> solutions between 5° and 80° C. The total volume of each dilatometer was approximately 130 ml and was known as a function of temperature. About 25 ml of mercury were

weighed into each dilatometer. After weighing, each dilatometer was filled with degassed solution and weighed again. The filled dilatometers were placed in a thermostat where the temperature was controlled and measured to a precision of  $\pm 0.001^\circ\text{C}$ . At approximately 5° C intervals, mercury was withdrawn from the dilatometer sidearms and weighed. Densities of mercury used were those reported by Beattie et al. (4). In this manner, changes of less than  $\pm 1 \times 10^{-4}$  ml out of a total of about 100 ml of solution could be detected. This corresponds to a precision of better than  $\pm 1$  ppm in the density of the solution as a function of temperature. As the initial weight of mercury and the weight of solution were determined in the procedure, absolute densities of the solutions were known to about  $\pm 5$ -10 ppm.

**Materials.** The solutions were prepared from the rare earth oxides and reagent grade HCl according to the method of Spedding et al. (46). This method results in solutions of the stoichiometric salt and also insures the removal of all colloidal material which tends to form in these solutions when prepared from the oxides. The resulting stock solutions were analyzed (46) by both cation and anion analyses to insure that equivalent amounts of rare earth and chloride ions were actually present. Secondary solutions were prepared by dilution with distilled water having a specific conductivity of about  $7 \times 10^{-7}$  ohm<sup>-1</sup> cm<sup>-1</sup>.

Highly purified mercury was obtained from the Special Materials Group of the Ames Laboratory of the Atomic Energy Commission. As a precaution against surface contaminants, the mercury was passed through a pinhole in filter paper before using, and the top layer of mercury in the funnel was discarded. Further details on the purity of the rare earth oxides and mercury and the methods of solution preparation and analysis are given elsewhere (21, 25).

## Calculations and Results

**Calibration of dilatometers.** As it was necessary to know the volume of each dilatometer as a function of temperature, the dilatometers were calibrated by use of mercury as the calibrating liquid. The calibrated dilatometers have been used to determine the densities of water from 5° to 80° C (22). To further insure consistency in the volume calibrations of the dilatometers between Series I and Series II, and from one dilatometer to another, the volume parameters of the dilatometers were refined by use of the average density of water data (22, 25), as obtained from all the dilatometers.

**Solutions.** The experimental densities and temperatures are given in Tables I-IV. A small loss of water from the solutions during the degassing procedure precluded precise knowledge of the solution concentrations. However, accurate pycnometric densities at 25° C are available for these solutions as a function of concentration (49). These pycnometric density data (49) were represented by polynomial expressions in the molality (25), and the concentrations of our solutions were obtained by substituting the densities of our solutions at exactly 25.000° C into these expressions and solving for the molality. For this purpose, the densities determined in this research were fitted as a function of temperature to Equation 1

<sup>1</sup> Present address, Department of Chemistry, Augustana College, Sioux Falls, S.D. 57102.

<sup>2</sup> To whom correspondence should be addressed.

$$d = \sum_{i=0}^5 C_i t^i \quad (1)$$

for each solution, and densities computed at 25.000°C. The concentrations obtained in this way are listed in Tables I-IV. The coefficients of Equation 1 are given in Table V, and the deviations from the experimental densities are given in Tables I-IV. Equation 1 fits the densities within the experimental precision in the density changes as a function of temperature and serves to represent accurately the densities as a function of temperature at the experimental concentrations.

Apparent molal volumes at the various temperatures were calculated from the experimental densities and concentrations according to

$$\phi_V = \frac{1000(d^\circ - d)}{m d^\circ d} + \frac{M_2}{d} \quad (2)$$

where  $M_2$  is the molecular weight of the solute (1969 IUPAC atomic weights), and  $m$  is the molal concentration. The densities of water,  $d^\circ$ , were calculated from (22)

$$d^\circ = 1 - \frac{(t - 3.9863)^2 (t + 288.9414)}{508929.2 (t + 68.12963)} + 0.0119893 \exp(-377.145/t) \quad (3)$$

The numerical values of the latter two coefficients in Equation 3 differ slightly from those given in ref. 22 owing to a minor refinement of the density of water data (25). This refinement involves an additional mercury calibration run with some of the dilatometers and a minor adjustment in the Mueller Bridge calibration, completed after the water density data had been published (25). These additional results were used in arriving at Equation 3. The differences in the densities as calculated from Equation 3 and those reported in ref. 22 are not significant. The apparent molal volumes calculated from Equation 2 are given in Tables I-IV. Some of the experimental  $\phi_V$  data are shown in Figures 1-3.

All the thermodynamic quantities derivable from  $\phi_V$  require derivatives of  $\phi_V$  with respect to concentration and/or temperature. The apparent molal volumes in Tables I-IV were therefore first fitted to

$$\phi_V = \sum_{i=0}^5 A_i t^i \quad (4)$$

for each concentration studied. These equations represent the temperature variation of  $\phi_V$  within 0.01 ml/mol at low concentrations to 0.001 ml/mol at high concentrations. The deviations of the experimental  $\phi_V$  values from Equation 4 are listed in Tables I-IV in column 5, and the coefficients of Equation 4 are given in Table VI.

Since graphs of the temperature coefficients in Equation 4 varied smoothly with concentration, the coefficients of each power in  $t$  were then fitted as functions of  $m^{1/2}$

$$A_i = \sum_{j=0}^4 B_{ij} m^{j/2} \quad (5)$$

which upon substitution into Equation 4 yields

$$\phi_V = \sum_i \sum_j B_{ij} m^{j/2} t^i \quad (6)$$

The coefficients in Equation 6 are given in Table VII. Equation 6 fits the experimental  $\phi_V$  data to within 0.05 ml/mol at low concentrations and to within 0.01 ml/mol at high concentrations. Apparent molal volumes calculated from Equation 6 are shown in Figures 4 and 5.

From Equation 6 and the appropriate temperature and concentration derivatives, together with the parameters in Table VII, the following thermodynamic quantities were calculated according to the standard relationships (26):

$$\bar{V}_2 = \phi_V + m \left( \frac{\partial \phi_V}{\partial m} \right)_{T,P,n_1} \quad (7)$$

$$\bar{V}_1 = \bar{V}_1^\circ - \frac{M_1 m^2}{1000} \left( \frac{\partial \phi_V}{\partial m} \right)_{T,P,n_1} \quad (8)$$

$$\phi_E = \left( \frac{\partial \phi_V}{\partial T} \right)_{P,n_1,n_2} \quad (9)$$

$$\bar{E}_2 = \phi_E + m \left( \frac{\partial \phi_E}{\partial m} \right)_{T,P,n_1} \quad (10)$$

$$\bar{E}_1 = \bar{E}_1^\circ - \frac{M_1 m^2}{1000} \left( \frac{\partial \phi_E}{\partial m} \right)_{T,P,n_1} \quad (11)$$

where  $M_1 = 18.0154$  g/mol is the molecular weight of water;  $\bar{V}_1^\circ = M_1/d^\circ$ ;  $\bar{E}_1^\circ = \alpha^\circ \bar{V}_1^\circ$ ; and  $\alpha^\circ = -1/d^\circ (\partial d^\circ / \partial t)$  is ob-

Table I. Density and  $\phi_V$  for  $\text{LaCl}_3$

$t, ^\circ\text{C}$	$d, \text{g/ml}$	$\Delta d \times 10^6$	$\phi_V, \text{ml/mol}$	$\Delta \phi_V \times 10^3$
		0.063471m		
20.128	1.012527	-0.5	19.008	6.2
25.052	1.011338	1.3	19.455	-16.3
30.034	1.009908	-0.6	19.741	7.7
34.999	1.008279	0.0	19.803	-3.2
39.980	1.006451	-2.1	19.747	32.1
45.070	1.004404	1.9	19.446	-28.0
49.931	1.002282	0.9	19.111	-12.4
54.998	0.999908	-0.3	18.653	6.0
60.316	0.997251	-0.8	18.048	10.9
65.456	0.994528	-0.5	17.351	5.3
70.331	0.991813	0.4	16.588	-6.4
74.816	0.989203	0.5	15.807	-5.7
79.571	0.986324	-0.3	14.878	3.8
		0.11651m		
20.091	1.024351	-0.1	20.045	-0.0
25.042	1.023115	0.3	20.535	-0.6
30.043	1.021647	-0.5	20.840	3.4
34.954	1.020010	0.5	20.958	-5.5

$t, ^\circ\text{C}$	$d, \text{g/ml}$	$\Delta d \times 10^6$	$\phi_V, \text{ml/mol}$	$\Delta \phi_V \times 10^3$
		0.11651m		
39.976	1.018147	-0.2	20.941	0.9
44.909	1.016145	-0.9	20.791	8.4
50.118	1.013860	1.6	20.474	-12.4
55.017	1.011553	-0.7	20.102	6.4
60.044	1.009042	-0.3	19.591	1.9
64.961	1.006448	0.2	18.991	-3.3
69.720	1.003813	-0.0	18.328	0.2
74.790	1.000878	0.1	17.517	1.1
79.387	0.998106	-0.0	16.687	-0.4
		0.31192m		
20.091	1.067173	-0.2	22.297	0.3
25.042	1.065795	0.7	22.773	-1.5
30.043	1.064208	-0.8	23.084	2.3
34.954	1.062478	0.1	23.230	-0.8
39.976	1.060539	0.1	23.244	-0.4
44.909	1.058481	0.3	23.135	-0.7
50.118	1.056150	0.1	22.901	0.1

(Continued on page 294)

Table I. Continued

$t, ^\circ\text{C}$	$d, \text{g/ml}$	$\Delta d \times 10^6$	$\phi_V, \text{ml/mol}$	$\Delta\phi_V \times 10^3$	$t, ^\circ\text{C}$	$d, \text{g/ml}$	$\Delta d \times 10^6$	$\phi_V, \text{ml/mol}$	$\Delta\phi_V \times 10^3$
		0.31192 <sub>m</sub>					1.7910 <sub>m</sub>		
55.017	1.053817	-0.4	22.577	1.3	39.976	1.350586	0.2	32.310	-0.1
60.044	1.051290	-0.0	22.144	-0.3	44.909	1.348161	-0.3	32.259	0.2
64.961	1.048692	-0.3	21.632	0.5	50.118	1.345522	-0.2	32.134	0.2
69.720	1.046065	0.9	21.051	-2.7	55.017	1.342965	-0.2	31.955	0.1
74.790	1.043143	-0.6	20.353	2.5	60.044	1.340267	0.4	31.713	-0.3
79.387	1.040393	0.1	19.639	-0.7	64.961	1.337553	0.5	31.424	-0.3
		0.65314 <sub>m</sub>			69.720	1.334854	-0.9	31.098	0.4
20.091	1.139414	-0.1	25.181	0.0	74.790	1.331903	0.4	30.701	-0.1
25.042	1.137809	0.3	25.610	-0.1	79.387	1.329158	-0.1	30.300	-0.0
30.043	1.136035	-0.1	25.891	-0.0			1.9840 <sub>m</sub>		
34.954	1.134151	-0.6	26.035	0.5	20.107	1.394055	0.0	32.558	-0.1
39.976	1.132090	0.6	26.059	-0.9	25.089	1.391837	0.0	32.827	0.1
44.909	1.129934	-0.3	25.978	0.6	30.074	1.389551	-0.6	33.004	0.2
50.118	1.127528	0.4	25.784	-0.3	35.051	1.387202	1.1	33.097	-0.5
55.017	1.125144	-0.3	25.513	0.4	40.003	1.384794	0.1	33.117	-0.1
60.044	1.122584	-0.0	25.147	-0.2	44.961	1.382315	-0.6	33.070	0.3
64.961	1.119970	-0.1	24.712	-0.0	49.848	1.379804	-1.3	32.962	0.6
69.720	1.117340	0.2	24.219	-0.3	54.999	1.377087	1.1	32.787	-0.4
74.790	1.114432	-0.0	23.622	0.3	60.157	1.374288	1.8	32.554	-0.8
79.387	1.111704	-0.0	23.016	-0.1	65.201	1.371473	-1.8	32.276	0.6
		0.91541 <sub>m</sub>			70.185	1.368621	-0.9	31.952	0.4
20.107	1.192888	-0.4	27.008	0.3	74.861	1.365879	1.4	31.607	-0.5
25.089	1.191121	0.6	27.399	-0.4	79.741	1.362939	-0.4	31.208	0.1
30.074	1.189227	0.6	27.651	-0.6			2.3367 <sub>m</sub>		
35.051	1.187213	-0.9	27.782	0.8	20.091	1.455023	0.1	33.969	-0.1
40.003	1.185098	-0.6	27.801	0.6	25.042	1.452715	0.0	34.210	0.1
44.961 <sup>a</sup>	1.182885	16.9	27.706	-15.9	30.043	1.450325	-0.5	34.370	0.1
49.848 <sup>a</sup>	1.180578	14.7	27.544	-13.8	34.954	1.447919	0.1	34.456	-0.1
54.999	1.178026	2.1	27.297	-1.9	39.976	1.445397	1.1	34.477	-0.4
60.157	1.175370	-0.2	26.958	0.1	44.909	1.442854	-0.6	34.438	0.2
65.201	1.172669	-2.0	26.551	1.8	50.118	1.440101	-0.5	34.338	0.2
70.185	1.169904	-0.9	26.077	0.9	55.017	1.437446	-0.4	34.193	0.1
74.861	1.167223	2.5	25.572	-2.3	60.044	1.434655	0.9	33.996	-0.4
79.741	1.164329	-0.9	24.991	0.8	64.961	1.431854	-0.2	33.760	-0.0
		1.2370 <sub>m</sub>			69.720	1.429078	0.1	33.492	-0.0
20.128	1.256166	-0.2	28.940	0.1	74.790	1.426045	-0.4	33.167	0.2
25.052	1.254260	0.3	29.284	-0.0	79.387	1.423231	0.2	32.838	-0.1
30.034	1.252230	0.1	29.511	-0.1			3.0675 <sub>m</sub>		
34.999	1.250108	0.6	29.629	-0.5	20.091	1.573615	-0.3	36.444	0.0
39.980	1.247879	-2.5	29.653	1.6	25.042	1.571137	1.4	36.640	-0.2
45.070	1.245509	1.5	29.582	-0.9	30.043	1.568572	-2.5	36.775	0.6
49.931	1.243151	0.7	29.438	-0.4	34.954	1.566006	2.0	36.850	-0.5
54.998	1.240599	0.1	29.214	-0.1	39.976	1.563313	-1.5	36.876	0.3
60.316	1.237819	-0.7	28.902	0.4	44.909	1.560613	1.7	36.853	-0.4
65.456	1.235036	-0.7	28.531	0.4	50.118	1.557687	0.3	36.785	-0.0
70.331	1.232312	0.5	28.117	-0.3	55.017	1.554867	-2.2	36.682	0.5
74.816	1.229730	0.4	27.689	-0.1	60.044	1.551908	0.6	36.538	-0.2
79.571	1.226916	-0.2	27.184	0.1	64.961	1.548940	0.4	36.364	-0.1
		1.5619 <sub>m</sub>			69.720	1.545998	1.1	36.166	-0.3
20.128	1.317658	-0.4	30.637	0.1	74.790	1.542785	-1.4	35.925	0.4
25.052	1.315616	0.9	30.943	-0.3	79.387	1.539806	0.5	35.680	-0.1
30.034	1.313466	-0.1	31.147	-0.0			3.3901 <sub>m</sub>		
34.999	1.311241	-0.0	31.252	-0.1	20.128	1.622919	0.1	37.375	-0.0
39.980	1.308927	-2.2	31.273	1.1	25.052	1.620381	-0.8	37.557	0.2
45.070	1.306483	1.4	31.210	-0.6	30.034	1.617761	2.2	37.683	-0.5
49.931	1.304066	1.4	31.081	-0.6	34.999	1.615082	-2.2	37.759	0.4
54.998	1.301463	-0.1	30.881	0.1	39.980	1.612337	-0.4	37.787	0.1
60.316	1.298641	-1.0	30.602	0.4	45.070	1.609463	1.4	37.774	-0.3
65.456	1.295827	-1.1	30.270	0.5	49.931	1.606649	1.2	37.724	-0.2
70.331	1.293080	1.2	29.900	-0.7	54.998	1.603640	-1.9	37.636	0.4
74.816	1.290481	0.1	29.518	0.1	60.316	1.600405	-0.3	37.508	0.0
79.571	1.287653	-0.2	29.069	0.1	65.456	1.597195	0.7	37.351	-0.2
		1.7910 <sub>m</sub>			70.331	1.594075	0.9	37.174	-0.2
20.091	1.359624	0.0	31.713	-0.1	74.816	1.591135	-1.1	36.988	0.3
25.042	1.357485	0.1	31.999	0.1	79.571	1.587949	0.3	36.768	-0.1
30.043	1.355248	-0.6	32.189	0.2					
34.954	1.352981	0.6	32.288	-0.4					

<sup>a</sup> Entry not used in the least-squares fits.

Table II. Density and  $\phi_V$  for  $\text{PrCl}_3$ 

$t, ^\circ\text{C}$	$d, \text{g/ml}$	$\Delta d \times 10^6$	$\phi_V, \text{ml/mol}$	$\Delta\phi_V \times 10^3$	$t, ^\circ\text{C}$	$d, \text{g/ml}$	$\Delta d \times 10^6$	$\phi_V, \text{ml/mol}$	$\Delta\phi_V \times 10^3$
0.10059m					0.85426m				
5.063	1.023557	-1.0	12.676	-0.8	5.063	1.190437	-0.6	20.437	-0.7
10.001	1.023146	2.0	14.062	1.1	10.001	1.189105	1.1	21.464	1.3
15.009	1.022423	0.6	15.129	-1.1	15.009	1.187594	0.2	22.276	0.4
20.039	1.021420	-1.6	15.923	4.4	20.039	1.185927	-0.5	22.896	-0.9
24.867	1.020226	-1.1	16.446	-2.4	24.867	1.184192	-1.0	23.334	-0.6
29.967	1.018738	-0.3	16.801	-1.7	29.967	1.182225	-0.4	23.652	-0.2
34.896	1.017099	1.0	16.968	-3.7	34.896	1.180198	0.9	23.833	-0.2
40.009	1.015202	1.1	16.991	1.0	40.009	1.177966	0.8	23.907	0.6
44.936	1.013200	0.6	16.873	3.1	44.936	1.175700	0.5	23.879	0.6
49.840	1.011048	-0.2	16.631	2.6	49.840	1.173333	-0.9	23.762	1.0
54.807	1.008714	-0.9	16.267	0.4	54.807	1.170830	-0.1	23.558	-0.9
60.376	1.005924	-1.7	15.733	4.7	60.376	1.167896	-1.2	23.239	-0.2
65.051	1.003449	0.5	15.161	-10.9	65.051	1.165336	0.8	22.896	-1.5
70.119	1.000631	1.7	14.456	-9.0	70.119	1.162459	0.8	22.458	0.1
75.041	0.997764	-0.6	13.701	20.3	75.041	1.159566	-0.6	21.967	2.3
79.578	0.995018	-0.1	12.871	-8.0	79.578	1.156816	0.0	21.457	-1.2
0.24985m					1.0718m				
5.063	1.057868	0.1	14.758	-4.7	5.043	1.235866	-0.1	22.000	-1.0
10.001	1.057243	-0.5	16.081	10.4	10.001	1.234327	0.4	22.945	1.6
15.009	1.056345	0.3	17.091	1.0	15.004	1.232640	-0.5	23.693	0.8
20.039	1.055200	2.1	17.839	-12.8	20.046	1.230814	-0.2	24.268	-1.0
24.867	1.053884	-2.0	18.377	2.4	24.868	1.228952	-0.2	24.676	-1.2
29.967	1.052296	-0.4	18.737	-0.2	29.996	1.226854	0.8	24.974	-1.1
34.896	1.050573	-0.8	18.933	5.4	34.926	1.224725	0.3	25.148	0.4
40.009	1.048610	0.6	18.981	2.5	40.035	1.222407	-0.4	25.222	1.4
44.936	1.046557	1.7	18.897	-2.8	44.939	1.220079	-0.0	25.200	0.9
49.840	1.044365	0.4	18.707	-1.4	49.927	1.217609	-1.7	25.094	1.4
54.807	1.042000	-1.5	18.409	2.5	54.940	1.215029	1.2	24.906	-1.8
60.376	1.039191	0.3	17.940	-5.9	60.461	1.212072	1.2	24.616	-2.0
65.051	1.036703	-1.2	17.468	2.6	64.990	1.209556	-1.0	24.318	0.3
70.119	1.033883	0.8	16.854	0.1	70.111	1.206621	0.4	23.914	0.4
75.041	1.031021	0.8	16.178	2.5	75.055	1.203691	-0.6	23.465	1.8
79.578	1.028280	-0.5	15.484	-1.6	79.504	1.200978	0.3	23.011	-1.2
0.42534m					1.3192m				
5.063	1.097374	-0.7	16.686	-1.1	5.043	1.286124	-0.2	23.605	-0.7
10.001	1.096520	1.5	17.912	1.6	10.001	1.284383	0.3	24.465	1.4
15.009	1.095423	-0.0	18.871	1.2	15.004	1.282517	0.7	25.148	-0.1
20.039	1.094110	-0.7	19.592	-1.3	20.046	1.280529	-0.7	25.678	-0.5
24.867	1.092666	-1.1	20.094	-1.0	24.868	1.278531	-1.4	26.056	-0.2
29.967	1.090960	-0.3	20.448	-0.4	29.996	1.276308	1.4	26.334	-1.2
34.896	1.089146	1.0	20.641	-0.6	34.926	1.274070	-0.4	26.500	0.8
40.009	1.087102	1.3	20.706	-0.1	40.035	1.271655	1.2	26.573	0.2
44.936	1.084984	-0.3	20.653	2.9	44.939	1.269244	0.1	26.560	0.7
49.840	1.082742	-0.5	20.491	1.3	49.927	1.266699	-2.0	26.471	1.3
54.807	1.080341	-0.1	20.227	-1.7	54.940	1.264056	0.8	26.306	-1.2
60.376	1.077497	-1.0	19.822	-0.6	60.461	1.261037	0.3	26.048	-1.1
65.051	1.074994	0.4	19.394	-2.2	64.990	1.258480	-0.2	25.781	-0.3
70.119	1.072163	1.2	18.849	-0.7	70.111	1.255501	0.4	25.419	0.4
75.041	1.069297	-0.7	18.245	4.9	75.055	1.252535	-0.5	25.016	1.4
79.578	1.066563	0.1	17.613	-2.4	79.504	1.249793	0.2	24.609	-0.8
0.63052m					1.5793m				
5.063	1.142486	-0.5	18.618	-1.1	5.043	1.337387	0.2	25.141	-0.8
10.001	1.141389	1.1	19.743	1.9	10.001	1.335458	-0.4	25.925	1.5
15.009	1.140083	-0.1	20.628	0.9	15.004	1.333425	0.4	26.550	0.1
20.039	1.138593	-0.4	21.299	-1.3	20.046	1.331286	-0.4	27.037	-0.5
24.867	1.137004	-0.9	21.770	-0.9	24.868	1.329158	-0.5	27.386	-0.6
29.967	1.135169	0.0	22.107	-0.8	29.996	1.326809	0.6	27.647	-0.6
34.896	1.133250	1.1	22.296	-0.6	34.926	1.324465	0.7	27.804	0.1
40.009	1.131114	0.6	22.369	1.0	40.035	1.321949	1.1	27.879	0.2
44.936	1.128923	-0.7	22.330	2.5	44.939	1.319449	-2.4	27.876	1.8
49.840	1.126624	-0.1	22.192	0.3	49.927	1.316829	-0.9	27.800	0.5
54.807	1.124174	-0.3	21.961	-1.0	54.940	1.314112	0.4	27.658	-0.8
60.376	1.121289	-0.7	21.602	-0.9	60.461	1.311025	2.9	27.430	-2.2
65.051	1.118761	1.0	21.220	-2.3	64.990	1.308410	-1.7	27.195	0.5
70.119	1.115910	0.5	20.733	0.5	70.111	1.305377	-0.0	26.874	0.5
75.041	1.113034	-0.9	20.189	3.6	75.055	1.302363	-0.5	26.515	1.1
79.578	1.110295	0.3	19.623	-1.9	79.504	1.299579	0.3	26.152	-0.8

(Continued on page 296)

Table II. Continued

$t, ^\circ\text{C}$	$d, \text{g/ml}$	$\Delta d \times 10^6$	$\phi_V, \text{ml/mol}$	$\Delta\phi_V \times 10^3$	$t, ^\circ\text{C}$	$d, \text{g/ml}$	$\Delta d \times 10^6$	$\phi_V, \text{ml/mol}$	$\Delta\phi_V \times 10^3$
		1.8419m					2.6963m		
5.043	1.387532	-0.1	26.569	-0.6	49.927	1.515096	-0.2	32.646	0.1
10.001	1.385441	0.1	27.286	1.1	54.940	1.511991	1.6	32.591	-0.8
15.004	1.383255	-0.2	27.861	0.3	60.461	1.508481	-0.6	32.485	-0.3
20.046	1.380978	0.5	28.311	-0.8	64.990	1.505533	-0.7	32.363	-0.0
24.868	1.378728	-0.5	28.637	-0.5	70.111	1.502125	0.5	32.191	0.2
29.996	1.376259	-0.3	28.883	-0.1	75.055	1.498757	-0.1	31.991	0.5
34.926	1.373813	0.5	29.033	0.2	79.504	1.495662	-0.0	31.783	-0.4
40.035	1.371198	0.5	29.109	0.5			2.9991m		
44.939	1.368614	0.1	29.113	0.5	5.043	1.590271	-0.2	31.721	-0.3
49.927	1.365908	-1.5	29.053	0.6	10.001	1.587670	0.6	32.232	0.6
54.940	1.363114	0.9	28.931	-0.9	15.004	1.584985	-0.7	32.651	0.3
60.461	1.359944	0.5	28.735	-0.9	20.046	1.582220	0.2	32.989	-0.4
64.990	1.357270	-0.7	28.528	-0.0	24.868	1.579513	-0.3	33.245	-0.4
70.111	1.354169	0.1	28.244	0.4	29.996	1.576569	0.7	33.451	-0.3
75.055	1.351095	0.1	27.926	0.7	34.926	1.573670	-0.4	33.594	0.3
79.504	1.348259	-0.1	27.603	-0.5	40.035	1.570595	0.3	33.689	0.4
		2.1350m			44.939	1.567574	0.5	33.736	0.2
5.043	1.441590	-0.0	28.041	-0.5	49.927	1.564426	-1.7	33.742	0.4
10.001	1.439339	0.2	28.694	0.9	54.940	1.561193	1.1	33.708	-0.6
15.004	1.437004	-0.1	29.221	0.2	60.461	1.557542	0.4	33.629	-0.5
20.046	1.434586	-0.2	29.636	-0.5	64.990	1.554477	-0.5	33.534	-0.1
24.868	1.432210	-0.7	29.939	-0.4	70.111	1.550936	0.1	33.394	0.3
29.996	1.429616	1.6	30.171	-0.8	75.055	1.547442	-0.1	33.229	0.5
34.926	1.427050	-0.7	30.318	0.5	79.504	1.544233	0.0	33.055	-0.3
40.035	1.424321	-0.0	30.399	0.6			3.2959m		
44.939	1.421631	0.4	30.413	0.3	5.043	1.637996	0.0	32.779	-0.3
49.927	1.418822	-1.7	30.372	0.6	10.001	1.635296	0.1	33.254	0.6
54.940	1.415929	1.0	30.275	-0.8	15.004	1.632507	-0.3	33.647	0.2
60.461	1.412653	1.3	30.112	-1.0	20.046	1.629629	0.0	33.968	-0.4
64.990	1.409894	-1.3	29.936	0.2	24.868	1.626810	-0.5	34.214	-0.3
70.111	1.406702	0.1	29.694	0.4	29.996	1.623743	1.4	34.416	-0.4
75.055	1.403540	0.1	29.420	0.6	34.926	1.620718	-0.5	34.562	0.3
79.504	1.400626	0.0	29.140	-0.5	40.035	1.617510	-0.4	34.665	0.5
		2.4606m			44.939	1.614359	0.8	34.723	0.1
5.043	1.499423	-0.1	29.541	-0.4	49.927	1.611077	-1.5	34.746	0.3
10.001	1.497023	0.5	30.133	0.7	54.940	1.607705	0.0	34.732	-0.3
15.004	1.494542	-0.6	30.614	0.4	60.461	1.603905	1.4	34.679	-0.7
20.046	1.491985	0.6	30.995	-0.7	64.990	1.600715	-0.5	34.607	-0.1
24.868	1.489478	-1.5	31.277	-0.1	70.111	1.597037	0.5	34.496	0.1
29.996	1.486751	1.1	31.497	-0.5	75.055	1.593410	-1.1	34.361	0.7
34.926	1.484062	1.0	31.641	-0.0	79.504	1.590087	0.5	34.215	-0.4
40.035	1.481206	-0.1	31.726	0.5			3.6233m		
44.939	1.478397	-0.4	31.752	0.5	5.043	1.688705	-0.2	33.864	-0.3
49.927	1.475470	-2.5	31.729	0.8	10.001	1.685889	0.4	34.309	0.5
54.940	1.472461	2.0	31.656	-1.0	15.004	1.682975	-0.1	34.680	0.1
60.461	1.469056	1.0	31.526	-0.8	20.046	1.679964	0.1	34.987	-0.4
64.990	1.466192	-1.1	31.383	0.1	24.868	1.677011	-0.7	35.227	-0.3
70.111	1.462881	0.6	31.182	0.2	29.996 <sup>a</sup>	1.673807	12.8	35.427	-2.5
75.055	1.459604	-0.7	30.953	0.8	34.926	1.670625	0.3	35.579	0.1
79.504	1.456589	0.3	30.717	-0.5	40.035	1.667261	0.5	35.692	0.2
		2.6963m			44.939	1.663957	0.8	35.763	0.1
5.043	1.539884	-0.1	30.540	-0.4	49.927	1.660519	-2.0	35.803	0.3
10.001	1.537395	1.1	31.093	0.5	54.940 <sup>a</sup>	1.657009	16.6	35.806	-3.5
15.004	1.534818	-2.8	31.545	0.9	60.461	1.653024	2.0	35.780	-0.8
20.046	1.532171	2.7	31.905	-1.2	64.990	1.649696	-1.3	35.731	0.1
24.868	1.529571	-0.5	32.175	-0.4	70.111	1.645868	0.1	35.647	0.2
29.996	1.526745	-0.2	32.389	-0.1	75.055	1.642102	0.1	35.540	0.4
34.926	1.523965	-0.3	32.532	0.3	79.504	1.638655	-0.1	35.420	-0.3
40.035	1.521015	0.4	32.621	0.4					
44.939	1.518114	-0.7	32.657	0.5					

<sup>a</sup> Entry not used in the least-squares fits.

Table III. Density and  $\phi_V$  for  $\text{NdCl}_3$ , Series I

$t$ , °C	$d$ , g/ml	$\Delta d \times 10^6$	$\phi_V$ , ml/mol	$\Delta\phi_V \times 10^3$	$t$ , °C	$d$ , g/ml	$\Delta d \times 10^6$	$\phi_V$ , ml/mol	$\Delta\phi_V \times 10^3$
0.10499 <sub>m</sub>					1.3173 <sub>m</sub>				
20.107	1.022859	0.2	15.083	-3.1	70.185	1.260700	-0.5	24.488	0.3
25.089	1.021616	-0.6	15.617	7.8	74.861	1.257857	0.5	24.122	-0.2
30.074	1.020153	0.2	15.943	-2.4	79.741	1.254804	-0.1	23.692	0.0
35.051	1.018488	-0.1	16.112	-0.7	1.6812 <sub>m</sub>				
40.003	1.016648	0.9	16.116	-9.4	20.128	1.358464	-0.3	26.446	0.1
44.961	1.014630	-0.1	15.998	1.5	25.052	1.356178	0.8	26.810	-0.2
49.848	1.012483	-0.4	15.746	5.3	30.034	1.353782	-0.4	27.078	0.1
54.999	1.010059	-2.3	15.365	22.6	34.999	1.351316	0.0	27.253	-0.1
60.157	1.007482	2.9	14.790	-28.5	39.980	1.348762	-1.8	27.348	0.8
65.201	1.004809	0.3	14.193	-3.8	45.070	1.346075	2.8	27.365	-1.2
70.185	1.002034	-1.5	13.498	14.7	49.931	1.343422	-1.6	27.319	0.8
74.861	0.999316	0.5	12.734	-2.9	54.998	1.340583	1.5	27.204	-0.7
79.741	0.996357	0.0	11.887	-1.1	60.316	1.337506	-1.7	27.022	0.7
0.29892 <sub>m</sub>					65.456	1.334449	0.3	26.785	-0.2
20.128	1.067446	-0.3	17.383	0.6	70.331	1.331469	0.3	26.511	-0.2
25.052	1.066058	0.7	17.919	-1.3	74.816	1.328657	0.1	26.218	0.1
30.034	1.064462	-0.1	18.280	-0.1	79.571	1.325605	-0.1	25.866	0.0
34.999	1.062694	0.1	18.478	-0.9	2.0853 <sub>m</sub>				
39.980	1.060751	-2.0	18.544	6.3	20.107 <sup>a</sup>	1.435241	21.8	28.318	-8.6
45.070	1.058608	1.4	18.465	-4.2	25.089	1.432697	-0.0	28.663	-0.0
49.931	1.056412	1.3	18.290	-3.7	30.074	1.430105	0.2	28.912	-0.0
54.998	1.053978	-0.5	18.009	1.8	35.051	1.427445	-0.3	29.083	0.1
60.316	1.051274	-0.9	17.601	2.6	40.003	1.424729	0.5	29.184	-0.2
65.456	1.048521	-0.4	17.107	1.0	44.961	1.421937	-0.4	29.221	0.1
70.331	1.045790	1.2	16.548	-4.0	49.848	1.419115	-0.4	29.201	0.2
74.816	1.043173	-0.4	15.970	1.9	54.999	1.416067	0.9	29.123	-0.3
79.571	1.040299	-0.0	15.274	-0.1	60.157	1.412932	-0.2	28.992	0.1
0.61510 <sub>m</sub>					65.201	1.409790	-0.3	28.814	0.1
20.128	1.138025	-0.4	20.108	0.4	70.185	1.406611	0.0	28.593	-0.0
25.052	1.136397	1.0	20.599	-1.1	74.861	1.403558	0.2	28.347	-0.0
30.034	1.134592	-0.3	20.943	0.3	79.741	1.400298	-0.1	28.053	0.0
34.999	1.132649	-0.1	21.145	-0.1	2.2675 <sub>m</sub>				
39.980	1.130559	-1.8	21.228	2.5	20.128	1.468633	-0.0	29.120	-0.0
45.070	1.128290	1.5	21.191	-2.1	25.052	1.466054	0.1	29.441	0.1
49.931	1.125996	0.6	21.064	-0.7	30.034	1.463378	0.1	29.684	-0.1
54.998	1.123480	0.1	20.838	-0.0	34.999	1.460645	0.0	29.854	-0.1
60.316	1.120708	-0.4	20.505	0.4	39.980	1.457836	-1.5	29.958	0.5
65.456	1.117905	-1.4	20.099	1.9	45.070	1.454898	2.5	30.001	-0.8
70.331	1.115142	1.2	19.635	-1.7	49.931	1.452017	-0.6	29.990	0.3
74.816	1.112505	0.2	19.150	-0.0	54.998	1.448943	-0.7	29.927	0.3
79.571	1.109618	-0.2	18.571	0.3	60.316	1.445635	-0.8	29.809	0.2
0.90093 <sub>m</sub>					65.456	1.442358	1.6	29.646	-0.6
20.107	1.199730	0.1	22.105	-0.2	70.331	1.439174	-0.0	29.453	0.0
25.089	1.197880	-0.4	22.563	0.7	74.816	1.436181	-0.8	29.241	0.3
30.074	1.195902	0.3	22.881	-0.4	79.571	1.432944	0.3	28.982	-0.1
35.051	1.193802	0.4	23.077	-0.6	2.7082 <sub>m</sub>				
40.003	1.191594	-0.5	23.164	0.4	20.107	1.546467	-0.3	30.904	0.0
44.961	1.189272	-0.5	23.152	0.6	25.089	1.543652	0.9	31.205	-0.1
49.848	1.186875	0.4	23.052	-0.3	30.074	1.540770	-0.5	31.437	0.1
54.999	1.184238	0.5	22.860	-0.4	35.051	1.537827	-1.0	31.606	0.2
60.157	1.181483	-0.5	22.586	0.3	40.003	1.534836	1.8	31.718	-0.5
65.201	1.178686	-0.2	22.242	0.1	44.961	1.531769	-1.0	31.781	0.3
70.185	1.175822	0.4	21.833	-0.4	49.848	1.528682	-0.5	31.797	0.2
74.861	1.173045	-0.2	21.391	0.4	54.999	1.525356	0.4	31.767	-0.1
79.741	1.170056	0.0	20.869	-0.1	60.157	1.521950	1.8	31.695	-0.5
1.3173 <sub>m</sub>					65.201	1.518542	-1.9	31.585	0.5
20.107	1.286196	0.1	24.567	-0.1	70.185	1.515107	-0.8	31.439	0.2
25.089	1.284085	-0.3	24.973	0.4	74.861	1.511820	1.7	31.270	-0.4
30.074	1.281877	0.2	25.261	-0.2	79.741	1.508317	-0.5	31.063	0.1
35.051	1.279573	0.2	25.444	-0.2	2.7550 <sub>m</sub>				
40.003	1.277188	0.3	25.533	-0.2	20.107	1.554485	2.1	31.085	-0.6
44.961	1.274705	-0.8	25.540	0.6	25.089	1.551648	-6.2	31.384	1.7
49.848	1.272171	0.0	25.470	0.1	30.074	1.548747	1.2	31.614	-0.3
54.999	1.269406	0.7	25.321	-0.4	35.051	1.545782	11.9	31.784	-3.1
60.157	1.266539	-0.2	25.102	0.0	40.003	1.542735	-9.4	31.906	2.4
65.201	1.263647	0.0	24.823	-0.1	44.961	1.539647	-3.4	31.970	0.9

(Continued on page 298)

Table III. Continued

$t, ^\circ\text{C}$	$d, \text{g/ml}$	$\Delta d \times 10^6$	$\phi_V, \text{ml/mol}$	$\Delta\phi_V \times 10^3$	$t, ^\circ\text{C}$	$d, \text{g/ml}$	$\Delta d \times 10^6$	$\phi_V, \text{ml/mol}$	$\Delta\phi_V \times 10^3$
		2.7550m					3.4149m		
49.848	1.536538	2.2	31.989	-0.5	40.003	1.649987	0.9	34.235	-0.2
54.999	1.533187	2.5	31.964	-0.6	44.961	1.646579	-2.4	34.325	0.5
60.157	1.529756	0.2	31.896	-0.1	49.848	1.643157	0.5	34.377	-0.1
65.201	1.526329	-0.1	31.790	-0.0	54.999	1.639476	1.1	34.395	-0.2
70.185	1.522869	-2.2	31.650	0.6	60.157	1.635714	-0.9	34.378	0.1
74.861	1.519563	1.4	31.487	-0.3	65.201	1.631971	0.4	34.329	-0.1
79.741	1.516040	-0.2	31.285	0.0	70.185	1.628206	0.2	34.249	-0.0
		3.4149m			74.861	1.624617	-0.4	34.147	0.1
20.107	1.662936	0.2	33.433	-0.1	79.741	1.620817	0.2	34.012	-0.1
25.089	1.659802	-0.3	33.709	0.1					
30.074	1.656593	-0.7	33.932	0.1					
35.051	1.653318	1.3	34.105	-0.3					

<sup>a</sup> Entry not used in the least-squares fits.

Table IV. Density and  $\phi_V$  for  $\text{NdCl}_3$ , Series II

$t, ^\circ\text{C}$	$d, \text{g/ml}$	$\Delta d \times 10^6$	$\phi_V, \text{ml/mol}$	$\Delta\phi_V \times 10^3$	$t, ^\circ\text{C}$	$d, \text{g/ml}$	$\Delta d \times 10^6$	$\phi_V, \text{ml/mol}$	$\Delta\phi_V \times 10^3$
		0.10108m					0.91022m		
5.056	1.024109	-0.6	11.719	-4.9	75.023	1.174872	0.6	21.454	1.0
10.015	1.023693	1.2	13.130	9.2	79.520	1.172118	-0.8	20.976	-0.3
15.027	1.022966	0.1	14.203	3.6			1.3059m		
20.067	1.021960	-0.3	14.991	-8.9	5.056 <sup>a</sup>	1.289203	-397.3	22.602	233.6
24.882	1.020765	-0.9	15.536	-5.0	10.015	1.287825	0.0	23.243	-0.4
30.029	1.019259	-0.2	15.909	-2.4	15.027	1.285921	0.2	23.950	0.8
34.908	1.017630	-0.2	16.102	8.4	20.067	1.283897	-0.5	24.501	0.4
40.044	1.015722	0.9	16.129	3.0	24.882	1.281866	0.2	24.898	-0.7
44.964	1.013719	0.4	16.027	5.3	30.029	1.279591	0.2	25.200	-0.6
49.941	1.011531	0.9	15.784	-7.8	34.908	1.277338	0.3	25.383	-0.2
54.879	1.009205	-0.4	15.443	-4.2	40.044	1.274869	0.7	25.477	0.0
60.380	1.006445	-1.3	14.936	2.0	44.964	1.272407	-2.0	25.485	1.7
63.745	1.004672	-1.2	14.560	4.9	49.941	1.269829	0.7	25.411	-0.2
70.085	1.001167	2.0	13.702	-12.2	54.879	1.267181	0.4	25.269	-0.5
75.023	0.998288	-0.0	12.964	14.4	60.380	1.264126	-0.5	25.034	-0.2
79.520	0.995563	-0.4	12.171	-5.5	63.745	1.262206	0.7	24.851	-0.8
		0.50654m			70.085	1.258476	-0.4	24.436	0.6
5.056	1.117657	-0.5	16.374	-1.3	75.023	1.255476	-0.1	24.047	0.6
10.015	1.116689	1.1	17.579	2.2	79.520	1.252670	0.1	23.646	-0.4
15.027	1.115493	-0.5	18.525	1.9			1.7019m		
20.067	1.114093	0.5	19.240	-3.2	5.056 <sup>a</sup>	1.369076	37.3	24.638	-23.4
24.882	1.112580	-0.6	19.744	-1.6	10.015	1.366967	-0.1	25.428	-0.2
30.029	1.110789	-0.9	20.113	0.6	15.027	1.364792	0.1	26.051	0.6
34.908	1.108938	0.5	20.317	0.3	20.067	1.362522	0.4	26.541	-0.2
40.044	1.106832	-0.0	20.403	2.4	24.882	1.360275	-0.3	26.899	-0.3
44.964	1.104677	0.8	20.367	0.5	30.029	1.357791	0.1	27.177	-0.4
49.941	1.102362	0.8	20.227	-1.2	34.908	1.355356	-0.7	27.351	0.4
54.879	1.099939	-0.2	19.993	-1.2	40.044	1.352712	0.3	27.449	0.2
60.380	1.097098	-1.9	19.630	1.3	44.964	1.350100	0.0	27.470	0.3
63.745	1.095291	-0.1	19.351	-1.3	49.941	1.347378	1.0	27.424	-0.4
70.085	1.091742	1.4	18.729	-1.0	54.879	1.344598	0.2	27.318	-0.3
75.023	1.088851	-0.1	18.163	3.0	60.380	1.341410	-0.6	27.132	-0.1
79.520	1.086126	-0.3	17.580	-1.4	63.745	1.339411	-1.2	26.986	0.4
		0.91022m			70.085	1.335549	1.2	26.645	-0.1
5.056	1.206463	0.1	19.694	-1.4	75.023 <sup>a</sup>	1.332350	-98.3	26.373	47.2
10.015	1.205043	-1.9	20.722	4.2	79.520	1.329555	-0.2	25.996	-0.0
15.027	1.203463	3.8	21.529	-3.0			2.0909m		
20.067	1.201720	0.7	22.158	-2.0	5.056	1.443491	-0.2	26.663	-0.5
24.882	1.199924	-4.7	22.609	2.8	10.015	1.441180	0.6	27.347	0.8
30.029	1.197881	0.6	22.938	-1.1	15.027	1.438775	-0.2	27.904	0.3
34.908	1.195819	1.0	23.133	-0.3	20.067	1.436288	-0.4	28.347	-0.4
40.044	1.193524	-0.3	23.226	1.7	24.882	1.433848	-0.1	28.675	-0.6
44.964	1.191215	0.1	23.215	1.0	30.029	1.431168	-0.1	28.935	-0.2
49.941	1.188771	2.7	23.113	-2.4	34.908	1.428559	0.4	29.104	0.1
54.879	1.186236	0.4	22.934	-1.3	40.044	1.425741	1.0	29.209	0.2
60.380	1.183290	-3.7	22.647	2.3	44.964	1.422968	-0.9	29.247	0.8
63.745	1.181432	-1.2	22.424	0.3	49.941	1.420094	-0.1	29.225	0.1
70.085	1.177808	2.6	21.918	-1.6	54.879	1.417169	-0.4	29.151	-0.2

Table IV. Continued

$t, ^\circ\text{C}$	$d, \text{g/ml}$	$\Delta d \times 10^6$	$\phi_V, \text{ml/mol}$	$\Delta\phi_V \times 10^3$	$t, ^\circ\text{C}$	$d, \text{g/ml}$	$\Delta d \times 10^6$	$\phi_V, \text{ml/mol}$	$\Delta\phi_V \times 10^3$
		2.0909 $m$					2.9045 $m$		
60.380	1.413827	0.2	29.009	-0.6	75.023	1.544061	-0.8	32.110	0.7
63.745	1.411737	0.4	28.894	-0.5	79.520	1.540759	0.1	31.940	-0.4
70.085	1.407706	0.5	28.622	0.2			3.1855 $m$		
75.023	1.404480	-0.9	28.364	1.0	5.056	1.634967	-0.1	31.353	-0.2
79.520	1.401478	0.3	28.092	-0.6	10.015	1.632149	0.1	31.866	0.5
		2.4915 $m$			15.027	1.629236	0.0	32.295	-0.2
5.056	1.516549	0.1	28.529	-0.5	20.067 <sup>a</sup>	1.626255	14.8	32.645	-3.9
10.015	1.514026	-0.2	29.139	0.9	24.882 <sup>a</sup>	1.623327	13.1	32.920	-3.6
15.027	1.511417	0.2	29.640	0.1	30.029	1.620113	-0.3	33.156	-0.4
20.067	1.508731	0.2	30.044	-0.5	34.908	1.617011	-0.2	33.325	0.1
24.882	1.506105	-0.5	30.348	-0.4	40.044	1.613674	0.7	33.454	0.2
30.029	1.503233	0.5	30.595	-0.3	44.964	1.610405	-0.3	33.535	0.4
34.908	1.500445	-0.4	30.763	0.4	49.941	1.607030	0.5	33.576	-0.0
40.044	1.497442	0.6	30.875	0.3	54.879	1.603612	-0.9	33.581	0.0
44.964	1.494496	-0.9	30.929	0.7	60.380	1.599727	0.8	33.545	-0.5
49.941	1.491450	0.7	30.932	-0.2	63.745	1.597307	-1.1	33.503	0.0
54.879	1.488357	0.1	30.889	-0.3	70.085	1.592669	1.0	33.384	-0.0
60.380	1.484829	-0.5	30.791	-0.3	75.023	1.588980	-0.5	33.256	0.5
63.745	1.482628	0.0	30.706	-0.3	79.520	1.585565	0.1	33.113	-0.3
70.085	1.478392	0.8	30.497	0.1			3.3601 $m$		
75.023	1.475009	-0.7	30.293	0.8	5.056	1.663230	-0.0	31.991	-0.3
79.520	1.471868	0.2	30.076	-0.5	10.015	1.660342	-0.2	32.486	0.7
		2.9045 $m$			15.027	1.657355	0.5	32.901	0.0
5.056	1.588230	-0.1	30.267	-0.4	20.067	1.654280	-0.1	33.246	-0.3
10.015	1.585524	-0.1	30.816	0.8	24.882	1.651275	-0.5	33.516	-0.3
15.027	1.582729	0.6	31.270	0.0	30.029	1.647990	0.2	33.748	-0.2
20.067	1.579855	0.5	31.642	-0.5	34.908	1.644805	0.1	33.918	0.2
24.882	1.577048	-1.4	31.927	-0.1	40.044	1.641379	0.5	34.052	0.3
30.029	1.573982	-0.5	32.164	-0.0	44.964	1.638025	-0.8	34.139	0.5
34.908	1.571011	0.8	32.331	0.0	49.941	1.634564	0.4	34.189	-0.0
40.044	1.567812	1.0	32.453	0.2	54.879	1.631061	0.4	34.204	-0.3
44.964	1.564678	-0.8	32.523	0.5	60.380	1.627080	-0.3	34.181	-0.3
49.941	1.561441	0.6	32.549	-0.1	63.745	1.624604	-0.6	34.148	-0.1
54.879	1.558159	-0.3	32.535	-0.2	70.085	1.619862	0.9	34.047	0.1
60.380	1.554422	-1.2	32.476	-0.1	75.023	1.616096	-0.4	33.935	0.5
63.745	1.552096	0.4	32.418	-0.4	79.520	1.612614	0.0	33.807	-0.3
70.085	1.547623	1.2	32.265	0.0					

<sup>a</sup> Entry not used in the least-squares fits.

tained from Equation 3. In addition, the coefficients of thermal expansion were calculated from (26)

$$\alpha = \frac{m\phi_E + 1000\alpha^0/d^0}{(mM_2 + 1000)/d} \quad (12)$$

Some of the results of these calculations are illustrated in Figures 6-8 for  $\bar{V}_2$ , Figures 9 and 10 for  $\bar{V}_1$ , Figures 11-14 for  $\alpha$ , Figures 15-17 for  $\phi_E$ , Figure 18 for  $\bar{E}_2$ , and Figure 19 for  $\bar{E}_1$ . A complete set of graphs appears in the dissertation of one of the authors (A.H.) (25), together with calculated values of all the properties at even temperature and concentration intervals.

Similar experimental work is in progress on other rare earth solutions which cover the 5-80°C temperature range. To compare the results for  $\text{LaCl}_3$  below 20°C to those of  $\text{PrCl}_3$ ,  $\text{NdCl}_3$ , and those now under investigation, Equation 6 has been extrapolated to 5°C for  $\text{LaCl}_3$ . Comparison of the extrapolation of Equation 6 for  $\text{NdCl}_3$ , Series I, to the actual measurements below 20°C from  $\text{NdCl}_3$ , Series II, indicates that such an extrapolation for  $\text{LaCl}_3$  is adequate for qualitative comparisons.

From Figures 4 and 5, at 25°C there is a relatively large change in slope in the  $\phi_V$  vs.  $m^{1/2}$  curves below 0.1 $m$ . In view of the absence of data below 0.1 $m$  at temperatures other than 25°C, an extrapolation of the data reported here

to infinite dilution was not warranted. It should be pointed out that Equation 6 does not describe the concentration dependence of  $\phi_V$  below 0.1 $m$  at 25°C nor, presumably, at other temperatures and should not be extrapolated below 0.1 $m$  at any temperature. However, above this concentration the  $\phi_V$  data are approximately linear in  $m^{1/2}$  (less so on the  $c^{1/2}$  scale), in qualitative agreement with Masson's (31) rule on the molal scale,

$$\phi_V = \phi_V^* + S_V^*m^{1/2} \quad (13)$$

It has been shown (35) that in the absence of dilute data, the constants  $\phi_V^*$  and  $S_V^*$  are useful in estimating unknown  $\phi_V^*$  values of electrolytes, and  $S_V^*$  is related to ion-ion interactions in concentrated solutions. We have therefore calculated  $\phi_V$  values at even temperatures from Equation 4 at each concentration and fitted these to the Masson equation (the  $m^{1/2}$  version). The constants are listed in Table VIII. The fit of Equation 13 is only qualitative, and for accurate  $\phi_V$  values, Equation 6 should be used. The  $\phi_V^*$  at 25°C are 2.0, 1.3, and 1.0 ml/mol higher than the  $\phi_V^0$  obtained from extrapolation of the dilute magnetic float data (46) for  $\text{LaCl}_3$ ,  $\text{PrCl}_3$ , and  $\text{NdCl}_3$ , respectively.

There is some interest in obtaining the dependence of  $\bar{E}_2^0$  of ions on their surface charge density (37). A perusal of Figures 15 and 16 shows that in view of the theoretical limiting



slope, an extrapolation of  $\phi_E$  from the concentrated region to infinite dilution would be uncertain. However, the curvature in  $\phi_E$  at low concentrations suggests that  $\phi_E$  for the rare earths may approach the limiting slope at very low concentrations. To obtain a crude estimate of  $\bar{E}_2^0$  at 25°C, we therefore included the theoretical limiting slope for  $\phi_V$ , as a function of temperature (35), in Equation 6 and refitted the data. The  $\phi_V^0$  obtained in this way at 25°C agreed with the  $\phi_V^0$  obtained from the dilute work (46) within 0.5 ml/mol.  $\phi_E$  calculated below 0.1M at 25°C is shown in Figures 15 and 16, and the  $\bar{E}_2^0$  obtained were 0.036, 0.046, and 0.046 ml/mol-deg for LaCl<sub>3</sub>, PrCl<sub>3</sub>, and NdCl<sub>3</sub>, respectively.

**Errors.** The absolute errors in the density measurements are approximately 5–10 ppm, owing mainly to errors in the total weights of solution, initial weights of mercury, the abso-

lute volumes of the dilatometers, and absolute accuracy of the temperature measurement. However, the error in the density as a function of temperature is about a factor of 10 less than this. The errors in  $\phi_V$  as a function of temperature owing to the errors in the densities range from  $\pm 0.01$  ml/mol at low concentrations to  $\pm 0.0005$  ml/mol at high concentrations. The above estimates of the errors in  $d$  and  $\phi_V$  as a function of temperature are consistent with the deviations of the experimental density and  $\phi_V$  data from Equations 1 and 4, which were derived at the fixed experimental concentrations of each solution.

The absolute errors in  $\phi_V$  owing to the concentration uncertainty can be no less than the errors in the pycnometric measurements at 25°C of Spedding et al. (49), upon which the concentrations are based. Spedding et al. (49) estimated

Table V. Density Parameters Corresponding to Equation 1

Molality	$C_0$	$C_1 \times 10^4$	$C_2 \times 10^6$	$C_3 \times 10^8$	$C_4 \times 10^{10}$	$C_5 \times 10^{18}$
LaCl <sub>3</sub>						
0.063471	1.0146315	0.25467	-7.38133	5.17893	-3.12782	8.9315
0.11651	1.0267109	0.06915	-7.03876	4.74659	-2.74241	7.4557
0.31192	1.0704868	-0.60098	-5.84148	3.45366	-1.80510	4.3833
0.65314	1.1441661	-1.57519	-4.32722	2.18289	-1.12358	2.7132
0.91541	1.1986384	-2.26453	-3.15104	1.02924	-0.41136	0.7135
1.2370	1.2628492	-2.84871	-2.48191	0.77902	-0.49260	1.5639
1.5619	1.3251697	-3.39446	-1.67665	-0.00750	0.08087	-0.5543
1.7910	1.3674743	-3.54476	-1.97740	1.05488	-1.06585	3.9410
1.9840	1.4023559	-3.88734	-1.10501	-0.57991	0.61838	-2.9520
2.3367	1.4638079	-4.14866	-1.09070	-0.10640	-0.07194	0.1586
3.0675	1.5831367	-4.52198	-1.10914	0.27440	-0.70470	3.1209
3.3901	1.6328220	-4.77924	-0.48743	-1.20989	0.78924	-2.5900
PrCl <sub>3</sub>						
0.10059	1.0236397	0.20925	-7.59392	5.84145	-3.82602	11.6218
0.24985	1.0582103	-0.35615	-6.52827	4.53018	-2.75858	7.7682
0.42534	1.0980001	-0.96707	-5.45813	3.35514	-1.93719	5.2760
0.63052	1.1434040	-1.59362	-4.44178	2.30162	-1.20587	2.9391
0.85426	1.1916356	-2.19133	-3.54073	1.43025	-0.63719	1.2174
1.0718	1.2372934	-2.68642	-2.89888	0.95701	-0.41016	0.6159
1.3192	1.2877833	-3.17606	-2.29113	0.43995	-0.06733	-0.6294
1.5793	1.3392586	-3.62312	-1.76918	-0.02415	0.25214	-1.8203
1.8419	1.3895850	-3.99498	-1.49530	0.03968	-0.09274	0.1850
2.1350	1.4438180	-4.35879	-1.16826	-0.35327	0.25238	-1.2165
2.4606	1.5018097	-4.67833	-1.04971	-0.33080	0.09381	-0.3256
2.6963	1.5423564	-4.84225	-1.20617	0.12423	-0.49845	2.5001
2.9991	1.5928615	-5.08355	-1.04212	-0.43726	0.14336	-0.0026
3.2959	1.6406806	-5.26375	-1.16035	-0.47145	0.27476	-0.4403
3.6233	1.6915001	-5.47493	-1.30952	-0.54287	0.56541	-1.7982
NdCl <sub>3</sub> , Series I						
0.10499	1.0251648	0.11775	-7.14408	4.72777	-2.50814	5.7341
0.29892	1.0708595	-0.66611	-5.69377	3.17802	-1.62358	4.0364
0.61510	1.1428782	-1.59685	-4.47691	2.41184	-1.41204	4.0823
0.90093	1.2057543	-2.37459	-3.30257	1.12698	-0.39352	0.3540
1.3173	1.2937029	-3.33704	-1.92255	-0.39195	0.78401	-3.8655
1.6812	1.3669585	-3.85981	-1.90039	0.67790	-0.74227	2.9873
2.0853	1.4447145	-4.46366	-1.22651	-0.36323	0.30847	-1.3317
2.2675	1.4784994	-4.61413	-1.53848	0.75208	-1.13525	5.2141
2.7082	1.5572045	-5.10318	-1.12975	-0.26237	0.07659	0.0353
2.7550	1.5648294	-4.57849	-3.56033	4.48112	-4.29469	15.5162
3.4149	1.6748087	-5.58324	-1.66718	0.41642	-0.43454	2.4083
NdCl <sub>3</sub> , Series II						
0.10108	1.0241915	0.20730	-7.60437	5.85654	-3.83733	11.6490
0.50654	1.1184120	-1.24349	-5.05662	2.93360	-1.62881	4.2119
0.91022	1.2077447	-2.36380	-3.46218	1.56573	-0.91716	2.6970
1.3059	1.2912929	-3.22963	-2.38801	0.64863	-0.34253	0.8392
1.7019	1.3710679	-3.93021	-1.64312	0.00974	0.06602	-0.5745
2.0909	1.4457810	-4.46087	-1.33659	-0.01613	-0.11270	0.4815
2.4915	1.5190625	-4.91404	-1.12046	-0.24360	0.03225	0.1967
2.9045	1.5909308	-5.28552	-1.10046	-0.35656	0.15357	-0.0135
3.1855	1.6377791	-5.50319	-1.13362	-0.58568	0.55842	-1.8015
3.3601	1.6661064	-5.62445	-1.28023	-0.36877	0.35865	-0.7901

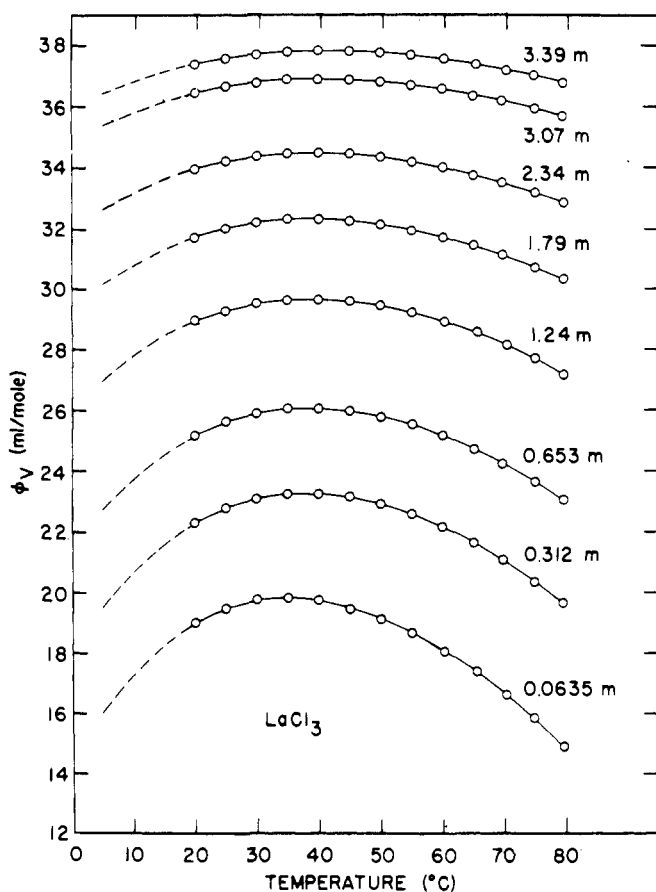


Figure 1. Apparent molal volume of  $\text{LaCl}_3$  as function of temperature. Circles, experimental; lines, Equation 4

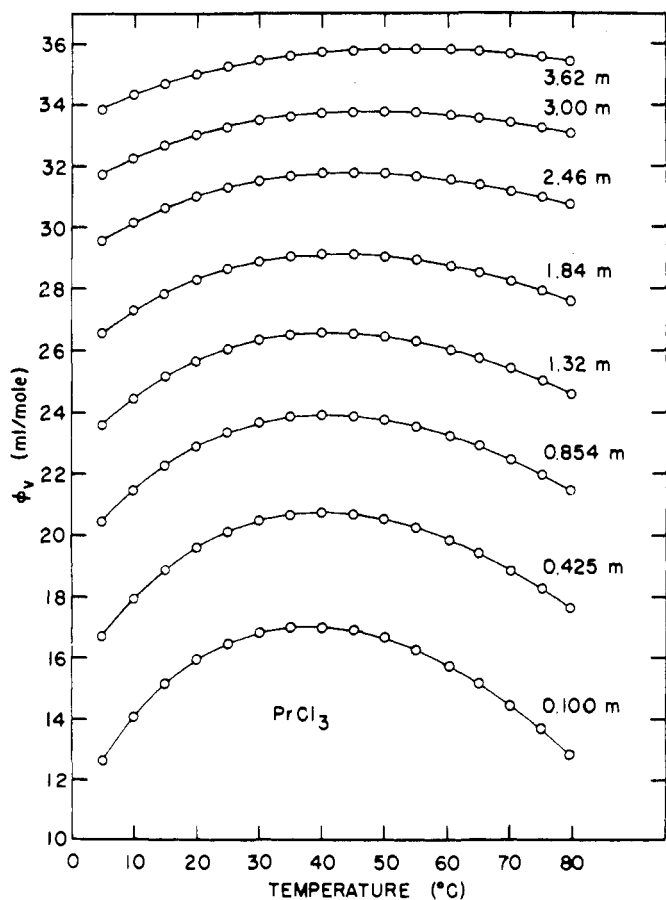


Figure 2. Apparent molal volume of  $\text{PrCl}_3$  as function of temperature. Circles, experimental; lines, Equation 4

their errors in  $\phi_V$  as ranging from  $\pm 0.2$  ml/mol at low concentration to  $\pm 0.1$  ml/mol at saturation. These estimates were based on an absolute analysis error of 0.05–0.1% in terms of the molality. However, since they made their dilutions by weight, the internal consistency of their concentrations was somewhat better than this. This internal consistency was preserved in the data treatment reported here.  $\phi_V$  values calculated from Equation 6 agree with the  $\phi_V$  data of the pycnometric work to within 0.05 ml/mol or better, as should be the case. Graphic illustration of this is given in Figures 4 and 5. And, as pointed out earlier, Equation 6, which necessarily includes the concentration errors, fits the  $\phi_V$  data presented here to within this error.

In obtaining the empirical equations, we endeavored to represent the data to within the precision of the particular independent variable at each step, to retain the internal consistency of the temperature and concentration variation. This approach is necessary since quantities such as  $\bar{E}_2$  and  $\bar{E}_1$  depend on the second derivative of  $\phi_V$ . However, because of the absolute analysis error, it should be kept in mind that the overall accuracy of  $\phi_V$  ranges from about 0.2 ml/mol at low concentrations to 0.1 ml/mol at 3.5 m at all temperatures. This error only becomes important when comparing  $\phi_V$  data of different rare earth solutions.

In this study it would be difficult to compute errors in properties which depend upon one or two derivatives of empirical equations. However, rough estimates are:  $\pm 0.2\%$  in  $\alpha$ ;  $\pm 0.5\%$  in  $\phi_E$  over most of the concentration range, but increasing in the familiar trumpet shape for apparent molal quantities (14) to as high as several % at the lowest concentrations; errors in  $\bar{V}_2$  and  $\bar{E}_2$  would be similar to those in  $\phi_V$  and  $\phi_E$  at low concentrations, becoming larger than those in  $\phi_V$  and  $\phi_E$  with increasing concentrations; errors in  $\bar{V}_1$  range from  $\pm 0.002\%$  for pure water to about  $\pm 0.1\%$  at high con-

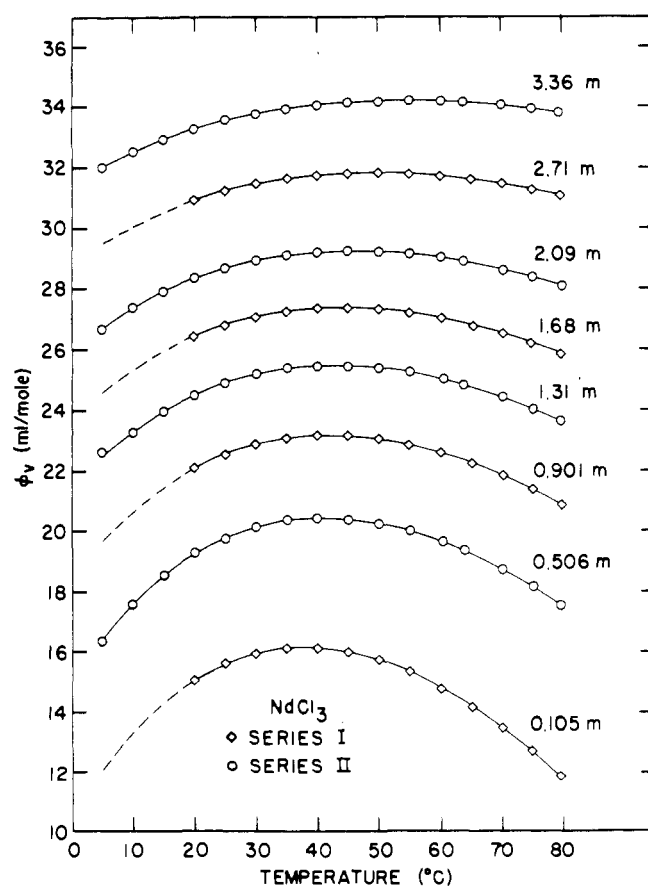


Figure 3. Apparent molal volume of  $\text{NdCl}_3$  as function of temperature. Circles and squares, experimental; lines, Equation 4

concentrations; and errors in  $\bar{E}_1$  are estimated at approximately  $\pm 0.2\%$  for pure water, increasing to  $\pm 0.5\%$  at high concentrations.

Alternatively, the results of this study can be compared with the results of independent measurements. The agreement between the results of this work and dilute magnetic float data (46) at 25°C is excellent as shown in Figures 4 and 5.  $\phi_E$  and  $\alpha$  obtained by Jones et al. (28) for LaCl<sub>3</sub> are compared to our values in Figures 11 and 15. The agreement is very good. The two independent data sets for NdCl<sub>3</sub> in this work were also worked up separately in addition to deriving the empirical equations for the combined sets of data. The results for the two separate NdCl<sub>3</sub> series agree within the errors quoted above.

Vogel observed that when a dilute, air-free solution of lanthanum chloride was added to his dilatometer, a small amount of white precipitate formed at the mercury-solution interface, identified as Hg<sub>2</sub>Cl<sub>2</sub> (56). This observation was confirmed for the 0.06348*m* LaCl<sub>3</sub> solution and after two to three weeks with the 0.1–0.3*m* LaCl<sub>3</sub> and NdCl<sub>3</sub> solutions. Qualitative and semiquantitative tests indicated that with the possible exception of the 0.06348*m* LaCl<sub>3</sub> solution, formation of Hg<sub>2</sub>Cl<sub>2</sub> or HgCl<sub>2</sub> caused little or no error in the measurements.

#### Discussion

Previous work in this laboratory has indicated that the number of inner sphere water molecules about the rare earth ions in dilute solutions and at 25°C remains constant from La to

Table VI. Apparent Molal Volume Parameters Corresponding to Equation 4

Molality	A <sub>0</sub>	A <sub>1</sub> × 10 <sup>1</sup>	A <sub>2</sub> × 10 <sup>3</sup>	A <sub>3</sub> × 10 <sup>5</sup>	A <sub>4</sub> × 10 <sup>7</sup>	A <sub>5</sub> × 10 <sup>9</sup>
LaCl <sub>3</sub>						
0.063471	14.4055	3.50600	-6.59624	2.12748	2.83801	-2.43281
0.11651	15.5044	3.50452	-7.21463	5.54787	-2.35995	0.14159
0.31192	17.9917	3.33046	-7.06776	6.54328	-4.14817	1.10688
0.65314	21.4338	2.85900	-5.85064	5.08807	-3.07358	0.79580
0.91541	23.5748	2.62588	-5.41838	4.77883	-2.91095	0.76587
1.2370	25.9485	2.26045	-4.50698	3.67711	-2.08031	0.50129
1.5619	27.9741	2.01198	-4.01625	3.31873	-1.95470	0.51117
1.7910	29.3153	1.78463	-3.38471	2.43045	-1.20982	0.25162
1.9840	30.2760	1.71825	-3.40393	2.83210	-1.75380	0.49795
2.3367	31.9550	1.50477	-2.90201	2.24551	-1.26460	0.32175
3.0675	34.8419	1.18353	-2.21452	1.61304	-0.81096	0.17430
3.3901	35.8839	1.10723	-2.13538	1.76497	-1.04171	0.27540
PrCl <sub>3</sub>						
0.10059	10.8501	4.06371	-9.55816	11.12494	-8.74073	2.88557
0.24985	13.0488	3.80277	-8.75475	10.20672	-8.18403	2.82019
0.42534	15.0951	3.52280	-7.90011	8.87645	-6.85143	2.27465
0.63052	17.1666	3.20442	-7.01017	7.63241	-5.77977	1.90108
0.85426	19.1191	2.90360	-6.21583	6.57397	-4.88874	1.58927
1.0718	20.8021	2.64163	-5.52478	5.63330	-4.10018	1.32273
1.3192	22.5197	2.38891	-4.90532	4.90101	-3.55216	1.15405
1.5793	24.1553	2.16583	-4.38115	4.32065	-3.12635	1.02275
1.8419	25.6722	1.96666	-3.88153	3.66580	-2.52713	0.78852
2.1350	27.2268	1.78278	-3.47180	3.29530	-2.30055	0.72925
2.4606	28.8065	1.60431	-3.05259	2.84595	-1.94527	0.60486
2.6963	29.8588	1.48482	-2.74752	2.47366	-1.61571	0.47566
2.9991	31.0932	1.36728	-2.51277	2.35471	-1.60237	0.48573
3.2959	32.1977	1.26226	-2.26545	2.14982	-1.48448	0.45010
3.6233	33.3232	1.17025	-2.03849	1.97654	-1.41309	0.43808
NdCl <sub>3</sub> , Series I						
0.10499	10.5443	3.45809	-7.10229	6.61265	-5.14345	1.92186
0.29892	12.6268	3.66840	-7.83809	7.62727	-4.79711	1.21922
0.61510	16.0173	3.05593	-5.99355	5.03931	-2.79248	0.62434
0.90093	18.4203	2.74379	-5.37582	4.75675	-2.96111	0.80832
1.3173	21.3665	2.37126	-4.61582	4.20691	-2.76943	0.81699
1.6812	23.6438	2.02416	-3.64140	2.76130	-1.42721	0.30762
2.0853	25.8586	1.76489	-3.10865	2.43076	-1.37359	0.34637
2.2675	26.7678	1.66517	-2.83764	2.01981	-0.93506	0.15775
2.7082	28.8001	1.47738	-2.49598	1.96880	-1.11619	0.27402
2.7550	29.1268	1.31374	-1.83452	0.72783	0.01369	-0.12349
3.4149	31.6403	1.21836	-1.88066	1.42642	-0.78074	0.16714
NdCl <sub>3</sub> , Series II						
0.10108	9.8982	4.06208	-9.44421	10.93269	-8.58395	2.84507
0.50654	14.8283	3.41904	-7.50233	8.30596	-6.38010	2.12312
0.91022	18.3950	2.85750	-5.93946	6.04844	-4.32431	1.35012
1.3059	21.2686	2.40274	-4.71296	4.35976	-2.88640	0.84679
1.7019	23.7038	2.08827	-4.00544	3.67988	-2.46369	0.74281
2.0909	25.8146	1.84759	-3.48427	3.24271	-2.21409	0.68130
2.4915	27.7765	1.63355	-2.99393	2.78176	-1.89707	0.57843
2.9045	29.5962	1.45258	-2.57834	2.41071	-1.65397	0.49960
3.1855	30.7273	1.35102	-2.35012	2.24655	-1.58533	0.48638
3.3601	31.3916	1.29257	-2.19791	2.08741	-1.47046	0.44613

Nd, decreases from Nd to Tb, and again remains constant from Tb to Lu (43, 46). Primary coordination numbers of nine and eight have been suggested (46). The volume properties of the rare earth chloride solutions from infinite dilution to saturation at 25°C have been reported (43, 46, 49) and discussed in terms of this hydration change and our present understanding of aqueous solutions containing small, highly charged ions. In what follows, we shall concentrate on how these properties change with temperature. It has been re-

ported that the hydration change probably occurs between Nd and Tb from infinite dilution to saturation (49), and all of the properties reported here change monotonically from La to Nd. Except for possibly a small fraction of 8-coordinated Nd ions, these three salts have predominantly the higher inner sphere coordination, and our concern with the hydration change will be minimal. Furthermore, we will attribute certain solution differences for La, Pr, and Nd solutions to differences in cation size, as a first approximation, since the chloride ion

Table VII. Matrix Coefficients,  $B_{ij}$ , Corresponding to Equation 6

$i$	$B_{0j}$	$B_{1j} \times 10$	$B_{2j} \times 10^3$	$B_{3j} \times 10^5$	$B_{4j} \times 10^7$	$B_{5j} \times 10^9$
LaCl <sub>3</sub>						
0	13.16045	3.281874	-6.366580	2.365504	1.899787	-1.967494
1	3.00208	2.204681	-7.569032	20.830004	-25.848852	12.190078
2	13.05398	-5.179800	16.111709	-34.762909	39.303245	-17.461539
3	-5.66861	2.588094	-8.691832	19.366320	-22.046183	9.764624
4	0.72472	-0.420563	1.551038	-3.658856	4.271842	-1.913151
PrCl <sub>3</sub>						
0	7.33653	4.211035	-10.416601	12.621156	-10.918243	3.969154
1	9.26902	0.632370	0.030499	-0.586084	3.977471	-2.590980
2	4.96866	-3.731125	9.007725	-12.711765	6.158433	-0.397690
3	-1.24015	1.915427	-5.327945	8.159326	-4.384721	0.510897
4	-0.08435	-0.299908	0.946806	-1.503887	0.750997	-0.051895
NdCl <sub>3</sub> , Series I and II						
0	7.01944	4.049902	-9.946627	11.914813	-10.041062	3.485562
1	6.47009	1.582629	-2.931885	4.765540	-1.908215	0.078915
2	8.58704	-5.389763	15.245779	-25.819582	20.774818	-6.738754
3	-3.41336	3.051321	-9.973919	18.594805	-16.146067	5.557504
4	0.41501	-0.561968	2.067342	-4.107507	3.699134	-1.310753

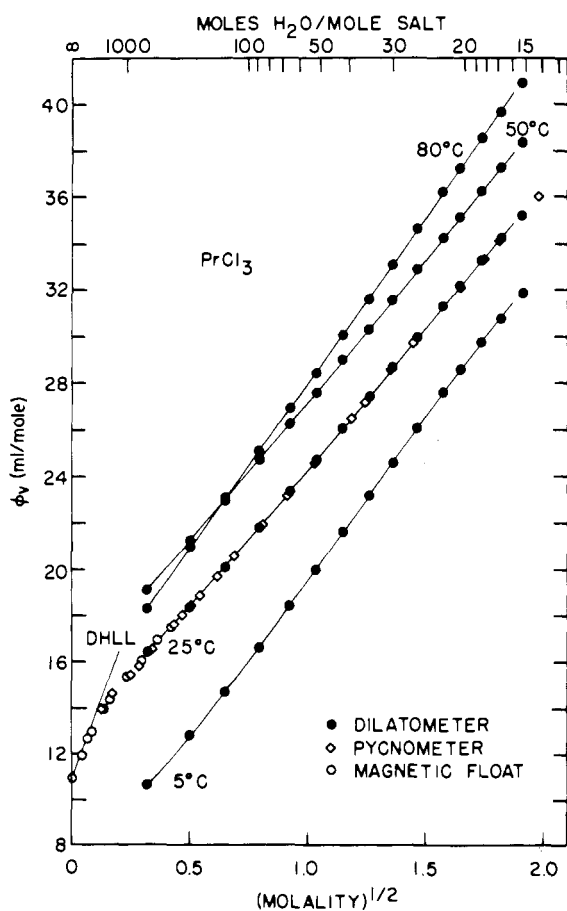


Figure 4. Apparent molal volume of PrCl<sub>3</sub> as function of square root of molality. Solid circles, Equation 4; lines, Equation 6. Ordinate applies only to 25°C curve. For ordinates at other temperatures, add 0.1 (25 -  $t$ ) ml

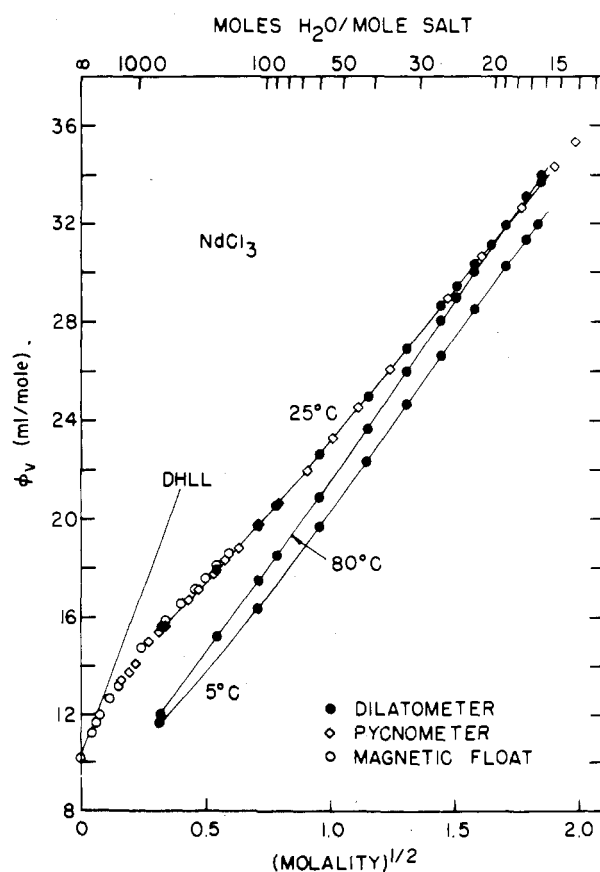


Figure 5. Apparent molal volume of NdCl<sub>3</sub> as function of square root of molality. Solid circles, Equation 4; lines, Equation 6

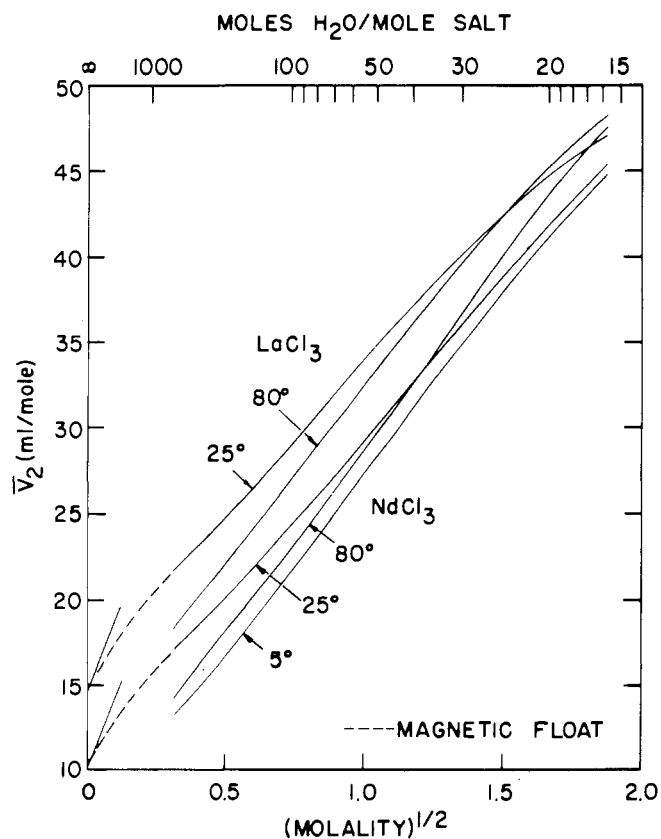


Figure 6. Partial molal volumes of  $\text{LaCl}_3$  and  $\text{NdCl}_3$  as functions of square root of molality. From Equation 7

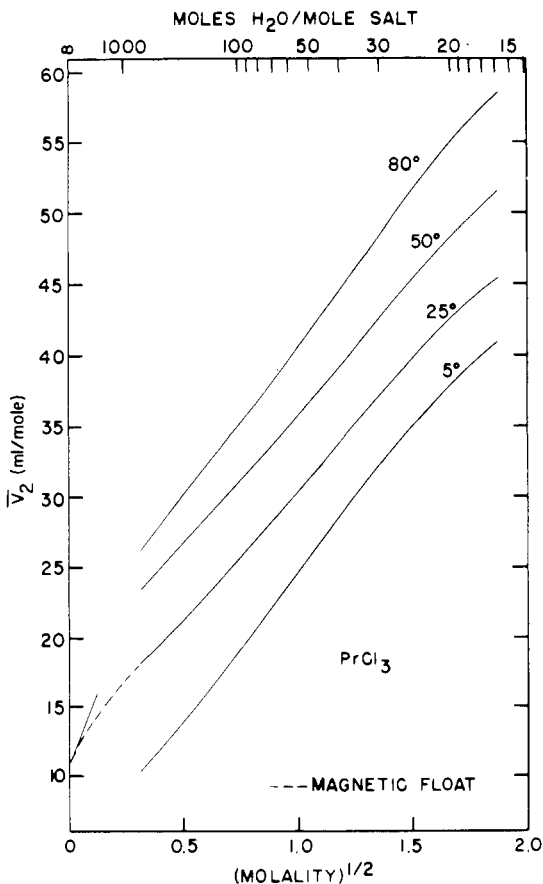


Figure 7. Partial molal volume of  $\text{PrCl}_3$  as function of square root of molality. From Equation 7. Ordinate applies only to  $25^\circ\text{C}$  curve. For ordinates at other temperatures, add  $0.2(25 - t)$  ml

is common to the three solutions, and the amount of complex formation between these cations and the chloride ion seems to be similar for these solutions (3, 5, 6, 23, 29, 39).

**Volume properties.** Because of the high surface charge density, the trivalent rare earth ions are highly electrostricting ions. The  $\bar{V}^0$  (ion) of the rare earth ions at  $25^\circ\text{C}$  and infinite dilution are  $-54.5$ ,  $-58.2$ , and  $-58.9$  ml/mol for La, Pr, and Nd, respectively (43). This increasing electrostriction from La to Nd is due to the decrease in ionic size (54) from La to Nd and is reflected in the decreasing  $\phi_V$ ,  $\bar{V}_2$ , and  $\bar{V}_1$  from La to Nd, which persists from 0.1 to 3.5 m at all temperatures in the results of this research (Figures 6, 8, and 9).

As can be seen in Figures 4–7,  $\phi_V$  and  $\bar{V}_2$  conform to the Debye-Hückel limiting law at  $25^\circ\text{C}$  if the very dilute data (46) are included. As mentioned earlier, above 0.1 m the increase in  $\phi_V$  and  $\bar{V}_2$  for the three salt solutions is approximately linear with the square root of the concentration at all temperatures, in qualitative agreement with Masson's (31) rule. However, from Figures 4–7, the slight S-shape with concentration is present for all three salts at all temperatures, particularly in  $\bar{V}_2$ . This slight S-shape is a rather common feature of  $\phi_V$  and  $\bar{V}_2$  curves in the concentrated ( $>0.1$  m) region of most simple salts (16, 30, 55). The Masson slopes for the rare earths are approximately 12, compared to about 8 for  $\text{CaCl}_2$  and 2 for  $\text{NaCl}$ , all on the molal scale (35).

As the concentration increases at a given temperature, a larger fraction of the available water undergoes electrostriction resulting in a decrease in  $\bar{V}_1$  with increasing concentration, as shown in Figure 9. This figure also shows that the degree of electrostriction of the water increases from La to Pr to Nd, at any given temperature and concentration.

Thus, the partial molal volumes of these solutions seem to

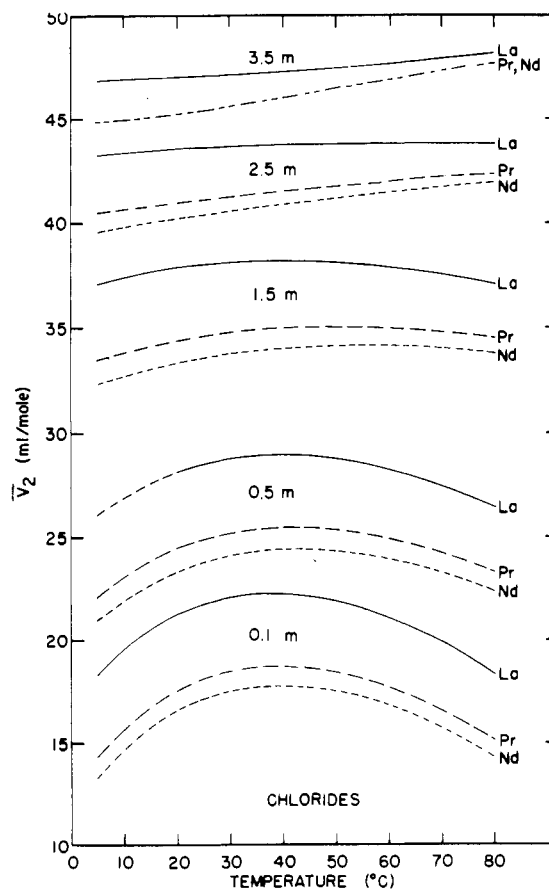


Figure 8. Partial molal volumes of  $\text{LaCl}_3$ ,  $\text{PrCl}_3$ , and  $\text{NdCl}_3$  as functions of temperature at several concentrations. From Equation 7

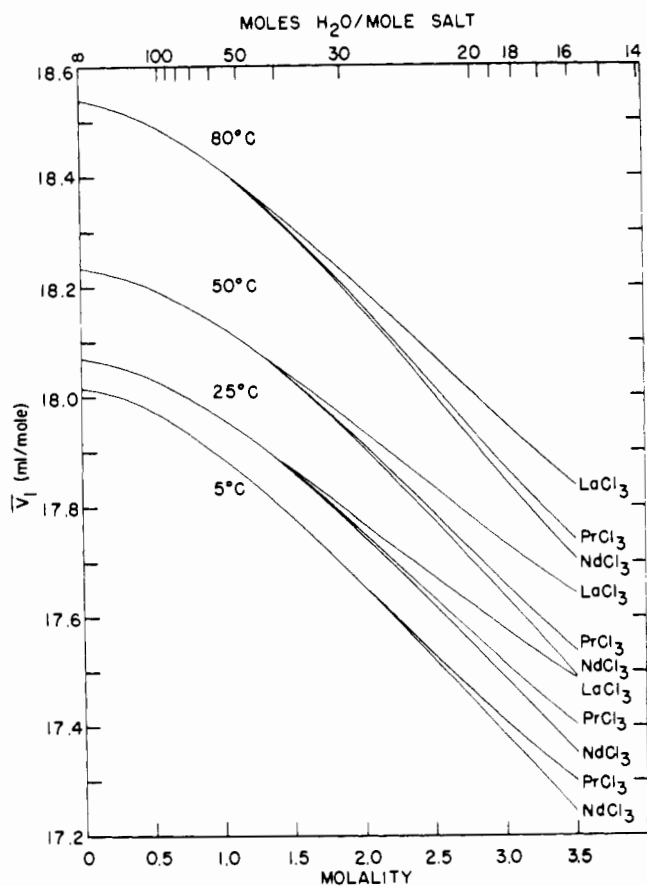


Figure 9. Partial molal volume of water in  $\text{LaCl}_3$ ,  $\text{PrCl}_3$ , and  $\text{NdCl}_3$  solutions as function of molality at several temperatures. From Equation 8

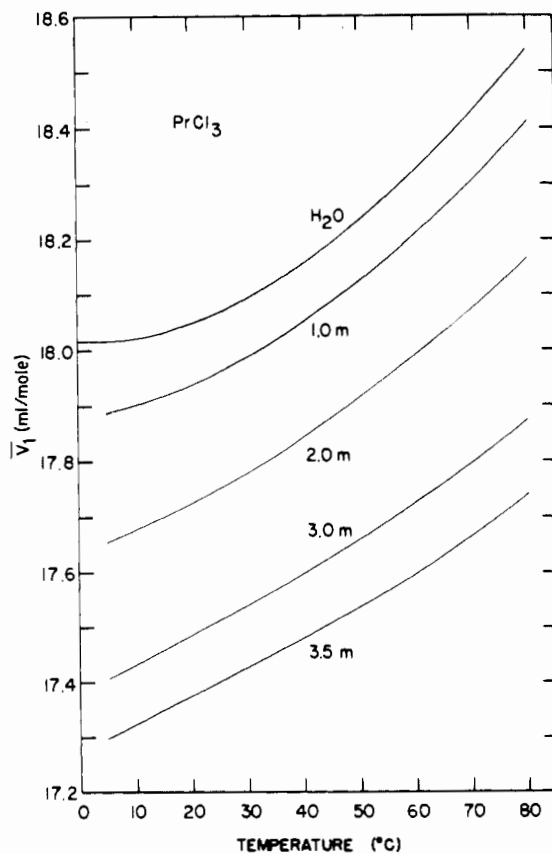


Figure 10. Partial molal volume of water in  $\text{PrCl}_3$  solutions as function of temperature at several concentrations. From Equation 8

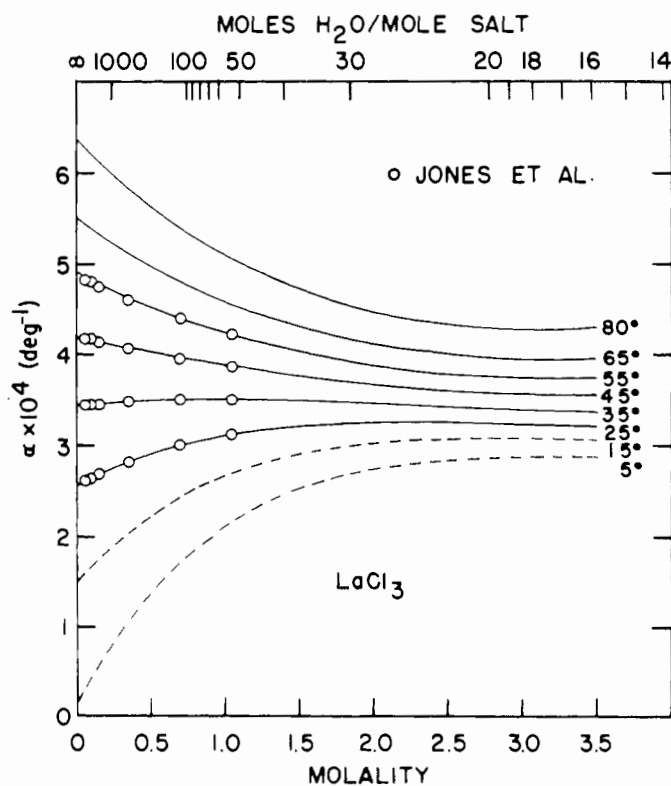


Figure 11. Coefficients of thermal expansion of  $\text{LaCl}_3$  solutions as function of molality at several temperatures. From Equation 12

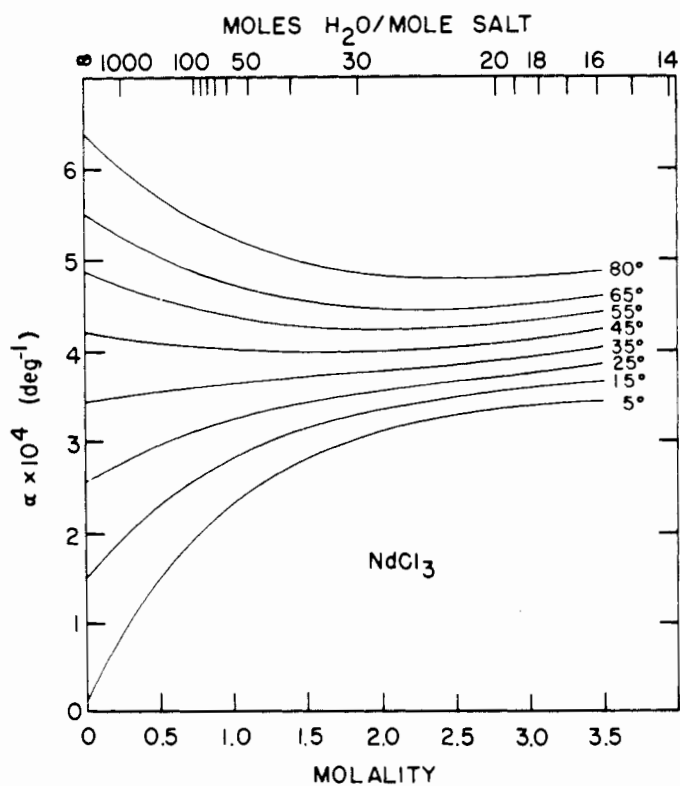


Figure 12. Coefficients of thermal expansion of  $\text{NdCl}_3$  solutions as function of molality at several temperatures. From Equation 12

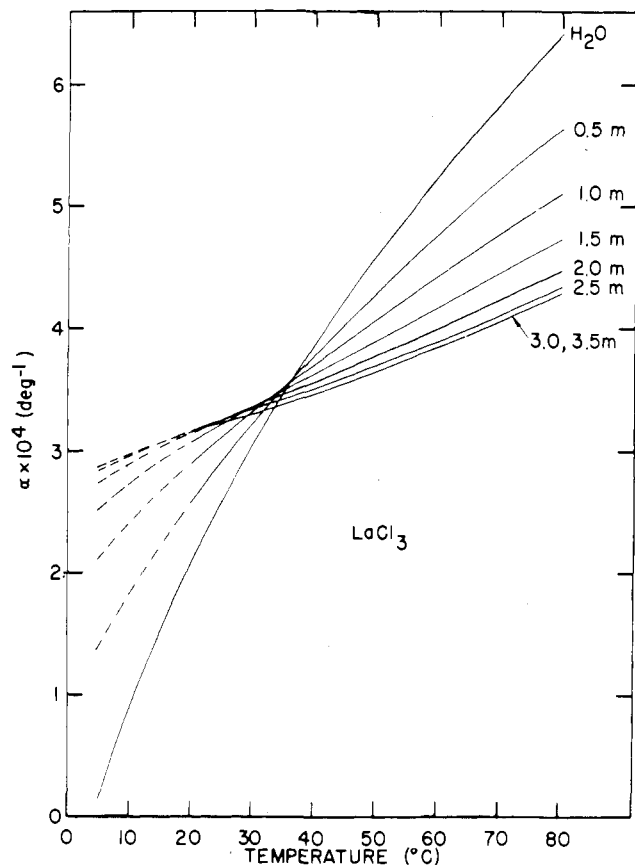


Figure 13. Coefficients of thermal expansion of  $\text{LaCl}_3$  solutions as function of temperature at several concentrations. From Equation 12

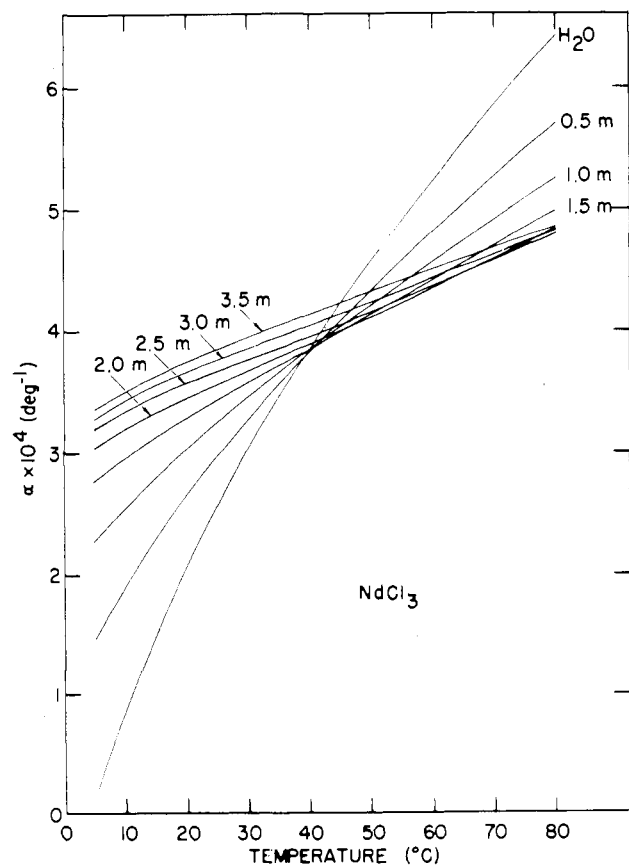


Figure 14. Coefficients of thermal expansion of  $\text{NdCl}_3$  solutions as function of temperature at several concentrations. From Equation 12

be in agreement with the trends expected from the surface charge density of the rare earth ions. The above considerations also apply to the volume properties of  $\text{YCl}_3$  at  $0^\circ$  and  $25^\circ\text{C}$  which have been reported previously (49).

From Figures 1-3 and 8,  $\phi_V$  goes through a maximum with temperature at all concentrations, as does  $\bar{V}_2$  up to approximately  $2.5m$ . The curvature becomes less pronounced with increasing concentration, disappearing altogether in  $\bar{V}_2$  above approximately  $2.5m$  where  $\bar{V}_2$  increases with temperature for the three cations. At  $0.1m$  the maxima in  $\phi_V$  occur at  $36.6^\circ$ ,  $38.3^\circ$ , and  $38.8^\circ \pm 0.5^\circ\text{C}$  for La, Pr, and Nd, respectively. At  $0.1m$  the maxima in  $\bar{V}_2$  occur  $1.2^\circ\text{C}$  higher than in  $\phi_V$ . In Figures 4 and 7 the  $\phi_V$  and  $\bar{V}_2$  curves at different temperatures have been separated (see figure captions) to show changes in the slopes of  $\phi_V$  and  $\bar{V}_2$  vs.  $m^{1/2}$  with increasing temperatures. These slopes decrease from  $5^\circ$  to somewhere between  $25^\circ$  and  $50^\circ\text{C}$  and then increase to  $80^\circ\text{C}$ . This can also be seen as the minimum (near  $35^\circ\text{C}$ ) in the Masson slopes as a function of temperature, Table VIII. Such changes in slope have been noted before (1, 7, 10-12, 14, 15, 55) and are equivalent to the flattening out of the  $\phi_V$  and  $\bar{V}_2$  vs.  $t$  curves.

Since such maxima occur at infinite dilution (7, 35), they must be due to ion-solvent interactions. At finite concentrations, ion-ion interactions complicate the situation. The origin of the maxima, even at infinite dilution, is by no means settled [see, for example, Millero (35) and Dunn (8)]. However, if the hydrogen-bonded solvent "structure" and its weakening with temperature are in part responsible for the maxima in the  $\phi_V$  and  $\bar{V}_2$  vs.  $t$  curves, as suggested by Dunn (7, 8), then the flattening out of the maxima and their eventual disappearance in  $\bar{V}_2$  at about  $2.5m$  ( $\sim 22$  waters/rare earth chloride unit), in-

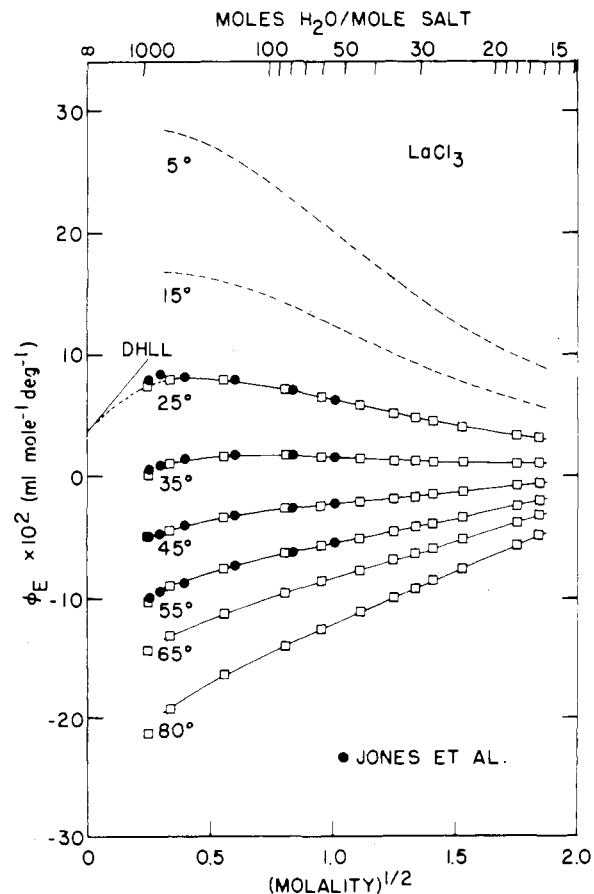


Figure 15. Apparent molal expansibility of  $\text{LaCl}_3$  as function of square root of molality at several temperatures. Squares, Equation 4; lines, Equation 9

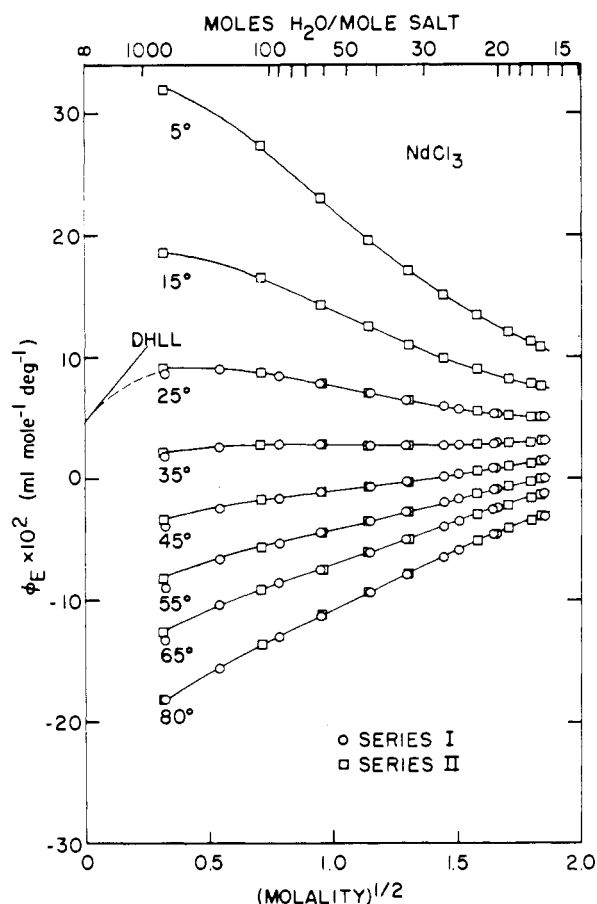


Figure 16. Apparent molal expansibility of  $\text{NdCl}_3$  as function of square root of molality at several temperatures. Squares and circles, Equation 4; lines, Equation 9

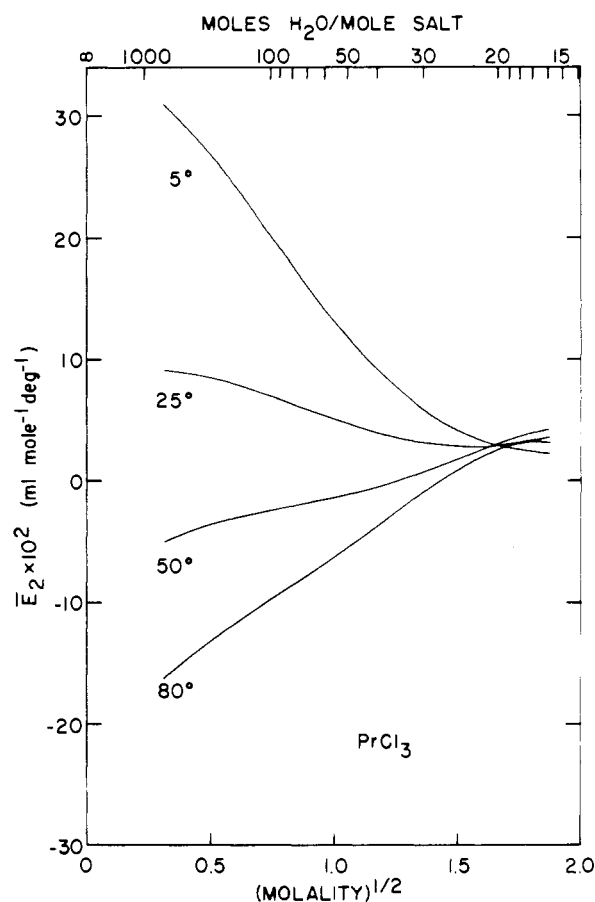


Figure 18. Partial molal expansibility of  $\text{PrCl}_3$  as function of square root of molality at several temperatures. From Equation 10

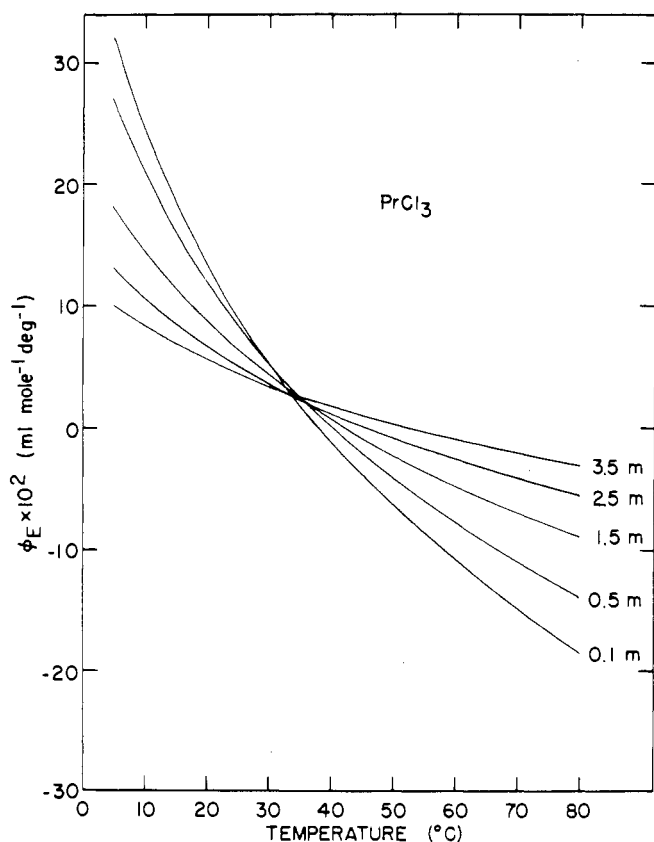


Figure 17. Apparent molal expansibility of  $\text{PrCl}_3$  as function of temperature at several concentrations. From Equation 9

indicate that little of the solvent structure remains in these solutions above this concentration. The variation of  $\bar{V}_1$  with temperature shown in Figure 10 seems to support this view. The curvature in the temperature dependence of the volume of water at infinite dilution (pure water) "straightens out" with increasing concentration, indicative of the reduction of the hydrogen-bonded solvent structure by the solute.

The maxima also seem to be a function of the surface charge density of the cations. For  $\text{NaCl}$  and  $\text{CaCl}_2$  which have cationic radii similar to the rare earth ions ( $\sim 1 \text{ \AA}$ ), the maxima occur at  $60^\circ$  and  $44^\circ\text{C}$ , respectively (35), at infinite dilution, compared to  $35\text{--}40^\circ\text{C}$  for the rare earth ions at  $0.1m$ . The  $\phi_E$  curves, Figures 15 and 16, indicate that at infinite dilution the maxima in the  $\phi_V^0$  vs.  $t$  curves (the temperature where  $\phi_E^0 = 0$ ) occur at even lower temperatures than at  $0.1m$  for the rare earth chloride solutions.

**Thermal expansion.** From elementary considerations and the simple Born model for ion-solvent interactions (37), one would expect the expansibility,  $E = dV/dT$ , to decrease upon the addition of an electrostricting solute, resulting in negative values for  $\phi_E^0 (= \bar{E}_2^0)$ . This effect should be greater with increasing surface charge density. Furthermore, with increasing concentration,  $\phi_E$  and  $\bar{E}_2$  should become less negative owing to the overlap of hydration spheres. This behavior is observed in solutions of electrolytes in nonaqueous solvents (19, 32) and in aqueous solutions at high temperatures, as shown in Figures 15, 16, and 18. However, in aqueous solutions at low temperatures, the expansibility increases with the addition of solute resulting in increasing  $\alpha$  and  $\bar{E}_1$ , and positive  $\phi_E$  and  $\bar{E}_2$  which decrease with concentration (14, 24, 28, 33, 36, 37). A study of the figures shows this to be true of these properties for the rare earths. The maxima in  $\phi_V$  with



temperature ( $d\phi_V/dT = \phi_E$ ) are of course related to this behavior.

The obvious and still viable rationalization for this effect was first put forward by Gibson and Loeffler (20). In terms of our modern understanding of pure water (9), the temperature dependence of the volume of pure water can be thought of as being due to two competing effects: the open, four-coordinate, hydrogen-bonded "structure" of water weakens with in-

creasing temperature, and the amplitude of the intermolecular vibrations increases with temperature. The second effect, the "vibrational" contribution, is dominant above 4°C and results in an increase in volume with heating, a positive  $dV/dT$  contribution. The first effect, the "configurational" contribution, is dominant below 4°C and results in a decrease in volume with heating, a negative  $dV/dT$  contribution. The balance of these two effects results in the minimum in the volume at 4°C and the great variation in  $\alpha^\circ$  with temperature.

The addition of an electrostricting solute at low temperatures greatly diminishes the (negative) configurational contribution to  $\alpha$  for those waters which end up in the hydration sphere. Although the expansibility of these waters in the hydration sphere would be low, it should be positive, the net result being an increase in  $\alpha$  and  $E_1$ , and positive  $\phi_E$  and  $\bar{E}_2$ . As the temperature increases, the configurational contribution in water is reduced owing to thermal action, and the effect of the solute upon the solvent is diminished. Assuming that the expansibility of the hydrated ion is less than the sum of the vibrational and configurational contributions of the solvent at high temperatures, the expansibility of the solvent decreases upon the addition of the electrostricting solute, resulting in decreasing  $\alpha$  and  $E_1$  and negative  $\phi_E$  and  $\bar{E}_2$  at high temperatures. Although this analysis is admittedly oversimplified, it does account for the major features in these properties. The expectation that these effects would be more pronounced for solutes of higher surface charge density is borne out by the results of this study.

Since pressure would also tend to weaken the hydrogen-bonded structure of water, it is not surprising that the pressure dependence of  $\alpha^\circ$  for pure water (9) bears a striking resemblance to the concentration dependence of  $\alpha$  for the rare earth solutions over the same temperature range. In this comparison, a 3.5m solution produces approximately the same effect as 3000–4000 atm external pressure on pure water. This analogy between the effect of an electrostricting solute and external pressure has been profitably explored by Gibson (17, 18).

Since  $\phi_E$  is approximately linear in  $m^{1/2}$  above the dilute region (similar to Masson's rule), there is a particular temperature where  $\phi_E$  is almost independent of concentration, as shown in Figures 15 and 16. The  $\phi_E$  vs.  $t$  curves from about 0.5 to 3m cross at this temperature as shown in Figure 17. The inversion temperatures in  $\phi_E$  are 37.5°, 36.3°, and 35.3°C for La, Pr, and Nd, respectively. At this temperature,

$$\frac{\partial \phi_E}{\partial m^{1/2}} = \frac{\partial \left( \frac{\partial \phi_V}{\partial m^{1/2}} \right)}{\partial T} = \frac{\partial S_V^*}{\partial T} = 0$$

i.e., the Masson slopes are at a minimum. This behavior appears also in  $\alpha$ , Figures 13 and 14, and in  $\bar{E}_2$  and  $\bar{E}_1$ , although the inversion temperature is less constant with concentration in these properties. Jones et al. (28) found the inversion temperature in  $\alpha$  at 37°C for  $\text{LaCl}_3$  (up to 1m) and at 52°C for  $\text{KCl}$  and  $\text{BaCl}_2$ . We obtain 36.5°C for  $\text{LaCl}_3$  in  $\alpha$  over the same concentration range. Therefore, the inversion temperature is also roughly a function of charge.

At high concentrations,  $\bar{E}_2$  converges on a value relatively insensitive to temperature and concentration, as shown in Figure 18. The results for  $\text{LaCl}_3$  and  $\text{NdCl}_3$  are similar. The low temperature and concentration dependence, as well as the small absolute value of  $\bar{E}_2$ , suggest that at these concentrations the solutions approach a quasicrystalline state (2, 13, 41, 57). It would be interesting to compare  $\alpha$  at these concentrations to the thermal expansion of the hydrated crystals, when these data become available.

Approach to the limiting law for  $\phi_E$  has been verified for  $\text{NaCl}$  from 0° to 50°C (14, 27, 36) and for  $\text{KCl}$  at 15°C (14). At all temperatures, the positive curvature in  $\phi_E$  vs.  $m^{1/2}$  for

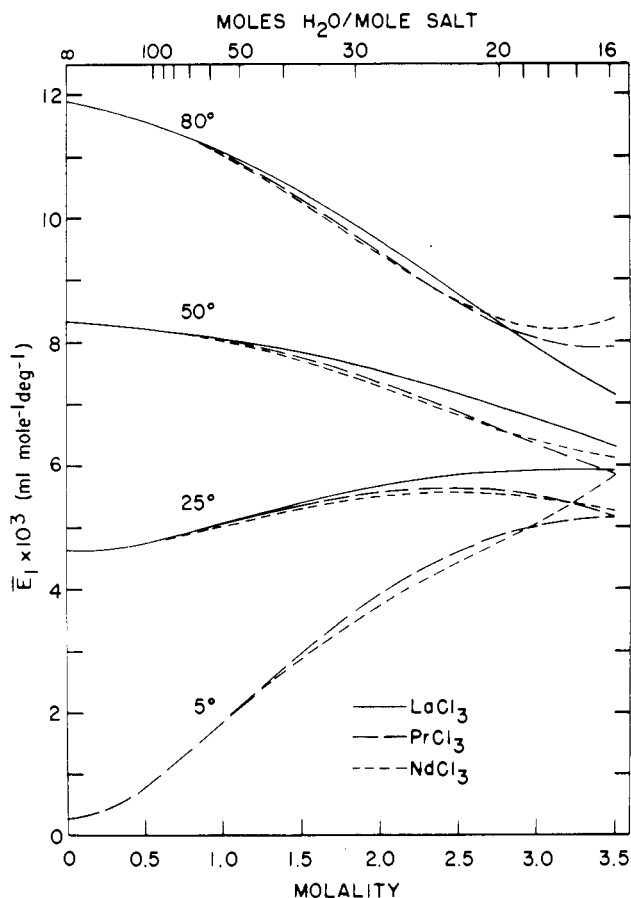


Figure 19. Partial molal expansibility of water in  $\text{LaCl}_3$ ,  $\text{PrCl}_3$ , and  $\text{NdCl}_3$  solutions as function of molality at several temperatures. From Equation 11

Table VIII. Parameters in Masson's Equation,  $\phi_V = \phi_V^* + S_V^* m^{1/2}$

$t, ^\circ\text{C}$	$\phi_V^*, \text{ml/mol}$			$S_V^*$		
	$\text{LaCl}_3$	$\text{PrCl}_3$	$\text{NdCl}_3$	$\text{LaCl}_3$	$\text{PrCl}_3$	$\text{NdCl}_3$
5		7.89	6.77		13.72	13.75
10		9.50	8.38		13.09	13.14
15		10.73	9.61		12.62	12.68
20	15.90	11.64	10.54	11.73	12.29	12.35
25	16.49	12.28	11.18	11.51	12.08	12.15
30	16.85	12.68	11.59	11.38	11.96	12.04
35	17.01	12.89	11.80	11.34	11.93	12.02
40	16.99	12.91	11.82	11.37	11.97	12.08
45	16.80	12.78	11.68	11.47	12.08	12.20
50	16.48	12.49	11.40	11.62	12.25	12.38
55	16.02	12.07	10.98	11.82	12.47	12.62
60	15.44	11.52	10.43	12.08	12.74	12.91
65	14.74	10.85	9.76	12.37	13.07	13.25
70	13.93	10.07	8.98	12.72	13.44	13.64
75	13.01	9.18	8.10	13.11	13.86	14.06
80	11.97	8.19	7.11	13.56	14.32	14.53

the rare earth chloride solutions at low concentrations suggests, but does not verify, approach to the Debye-Hückel limiting law. Measurements at much lower concentrations are needed, especially at low temperatures, where the deviations would be largest.

From the provisional  $\bar{E}_2^0$  at 25°C obtained earlier, and using the value of 0.046 ml/mol-deg for  $\bar{E}^0$  (Cl<sup>-</sup>) (37), we obtain  $\bar{E}^0$  (ion) = -0.102, -0.092, and -0.092 ml/mol-deg for La<sup>3+</sup>, Pr<sup>3+</sup>, and Nd<sup>3+</sup>, respectively. Using the same value for Cl<sup>-</sup>, Millero (37) obtained 0.032 ml/mol-deg for Na<sup>+</sup> and -0.042 ml/mol-deg for Ca<sup>2+</sup>. Thus,  $\bar{E}^0$  (ion) decreases with increasing charge as expected. However, the  $\bar{E}^0$  (ion) for the rare earths seems to decrease with increasing ionic radii, similar to the monovalent cations, but opposite the divalent cations (37). This implies that the smaller Pr and Nd ions decrease the expansibility of the solution less than the larger La ion. Considering the uncertainty in the extrapolation and the small range in radii (0.07 Å), this result must be treated with caution. Nevertheless,  $\alpha$ ,  $\phi_E$ , and  $\bar{E}_2^0$  all consistently increase from LaCl<sub>3</sub> to NdCl<sub>3</sub> over the whole temperature and concentration range. The extension of these measurements to lower concentrations and over a greater range of radii should clarify this point.

#### Acknowledgment

The authors thank the Ames Laboratory Rare Earth Separation Group for furnishing the oxides. They are also indebted to J. A. Rard for many helpful discussions.

#### Literature Cited

- (1) Akerlof, G., Teare, J., *J. Am. Chem. Soc.*, **60**, 1226 (1938).
- (2) Bahe, L. W., *J. Phys. Chem.*, **76**, 1062 (1972).
- (3) Bansal, B. M. L., Patil, S. K., Sharma, H. D., *J. Inorg. Nucl. Chem.*, **26**, 993 (1963).
- (4) Beattie, J. A., Blaisdell, B. E., Kaye, J., Gerry, H. T., Johnson, C. H., *Proc. Am. Acad. Arts Sci.*, **74**, 371 (1941).
- (5) Choppin, G. R., Unrein, P. I., *J. Inorg. Nucl. Chem.*, **25**, 387 (1963).
- (6) Connick, R. E., Mayer, S. W., *J. Am. Chem. Soc.*, **73**, 1176 (1951).
- (7) Dunn, L. A., *Trans. Faraday Soc.*, **64**, 2951 (1968).
- (8) Dunn, L. A., *J. Solution Chem.*, **3**, 1 (1974).
- (9) Eisenberg, D., Kauzmann, W., "The Structure and Properties of Water," Oxford Univ. Press, New York, N.Y., 1969.
- (10) Ellis, A. J., *J. Chem. Soc. (A)*, **1966**, p 1579.
- (11) Ellis, A. J., *ibid.*, **1967**, p 660.
- (12) Fabuss, B. M., Korosi, A., Shamsul Hug, A. K. M., *J. Chem. Eng. Data*, **11**, 325 (1966).
- (13) Frank, H. S., Thompson, P. T., in "The Structure of Electrolytic Solutions," W. J. Hamer, Ed., Wiley, New York, N.Y., 1959.
- (14) Franks, F., Smith, H. T., *Trans. Faraday Soc.*, **63**, 2586 (1967).
- (15) Geffcken, W., *Z. Phys. Chem.*, **A155**, 1 (1931).
- (16) Geffcken, W., Kruis, A., Solana, L., *Z. Phys. Chem.*, **B35**, 317 (1937).
- (17) Gibson, R. E., *J. Am. Chem. Soc.*, **56**, 4 (1934).

- (18) Gibson, R. E., *ibid.*, **57**, 284 (1935).
- (19) Gibson, R. E., Kincaid, J. F., *ibid.*, **59**, 579 (1937).
- (20) Gibson, R. E., Loeffler, O. H., *ibid.*, **63**, 443 (1941).
- (21) Gildseth, W. M., PhD dissertation, Iowa State University, Ames, Iowa, 1964.
- (22) Gildseth, W. M., Habenschuss, A., Spedding, F. H., *J. Chem. Eng. Data*, **17**, 402 (1972).
- (23) Goto, T., Smutz, M., *J. Inorg. Nucl. Chem.*, **27**, 663 (1965).
- (24) Gucker, F. T., *J. Am. Chem. Soc.*, **56**, 1017 (1934).
- (25) Habenschuss, A., PhD dissertation, Iowa State University, Ames, Iowa, 1973.
- (26) Harned, H. S., Owen, B. B., "The Physical Chemistry of Electrolytic Solutions," 3rd ed., Reinhold, New York, N.Y., 1958.
- (27) Jain, D. V. S., Lark, B. S., *Ind. J. Chem.*, **8**, 1133 (1970).
- (28) Jones, G., Taylor, E. F., Vogel, R. C., *J. Am. Chem. Soc.*, **70**, 966 (1948).
- (29) Kozachenko, N. N., Batyaev, I. M., *Russ. J. Inorg. Chem.*, **16** (1), 66 (1971).
- (30) Kruis, A., *Z. Phys. Chem.*, **B34**, 1 (1936).
- (31) Masson, D. O., *Phil. Mag., Ser. 7*, **8**, 218 (1929).
- (32) Millero, F. J., *J. Phys. Chem.*, **72**, 3209 (1968).
- (33) Millero, F. J., *J. Chem. Eng. Data*, **15**, 562 (1970).
- (34) Millero, F. J., *ibid.*, **16**, 229 (1971).
- (35) Millero, F. J., in "Water and Aqueous Solutions," R. A. Horne, Ed., Chap. 13, 14, Wiley-Interscience, New York, N.Y., 1972.
- (36) Millero, F. J., *J. Phys. Chem.*, **74**, 356 (1970).
- (37) Millero, F. J., *ibid.*, **72**, 4589 (1968).
- (38) Millero, F. J., *J. Solution Chem.*, **2**, 1 (1973).
- (39) Peppard, D. F., Mason, G. W., Hucher, I., *J. Inorg. Nucl. Chem.*, **24**, 881 (1962).
- (40) Rard, J. A., Spedding, F. H., *J. Phys. Chem.*, **79**, 257 (1975).
- (41) Rosen, J. S., NASA Technical Note, TN D-4297, 1968.
- (42) Spedding, F. H., Csejka, D. A., DeKock, C. W., *J. Phys. Chem.*, **70**, 2423 (1966).
- (43) Spedding, F. H., Cullen, P. F., Habenschuss, A., *ibid.*, **78**, 1106 (1974).
- (44) Spedding, F. H., Jones, K. C., *ibid.*, **70**, 2450 (1966).
- (45) Spedding, F. H., Pikal, M. J., *ibid.*, p 2430.
- (46) Spedding, F. H., Pikal, M. J., Ayers, B. O., *ibid.*, p 2440.
- (47) Spedding, F. H., Rard, J. A., *ibid.*, **78**, 1435 (1974).
- (48) Spedding, F. H., Rard, J. A., Saeger, V. W., *J. Chem. Eng. Data*, **19**, 373 (1974).
- (49) Spedding, F. H., Saeger, V. W., Gray, K. A., Boneau, P. K., Brown, M. A., DeKock, C. W., Baker, J. L., Shiers, L. E., Weber, H. O., Habenschuss, A., *ibid.*, **20**, 72 (1975).
- (50) Spedding, F. H., Shiers, L. E., Brown, M. A., Derer, J. L., Swanson, D. L., Habenschuss, A., *ibid.*, p 81.
- (51) Spedding, F. H., Shiers, L. E., Rard, J. A., *ibid.*, p 66.
- (52) Spedding, F. H., Shiers, L. E., Rard, J. A., *ibid.*, p 88.
- (53) Spedding, F. H., Witte, D., Shiers, L. E., Rard, J. A., *ibid.*, **19**, 369 (1974).
- (54) Templeton, D. H., Dauben, C. H., *J. Am. Chem. Soc.*, **76**, 5237 (1954).
- (55) Vaslow, F., *J. Phys. Chem.*, **70**, 2286 (1966).
- (56) Vogel, R. C., PhD thesis, Harvard University, Cambridge, Mass., 1946.
- (57) Wright, R., *J. Chem. Soc. London*, **1940**, p 870.

Received for review October 23, 1974. Accepted April 18, 1975. Report prepared for the U.S. Energy Research and Development Administration under Contract No. W-7405-eng-82, and based in part on the PhD dissertations of W.M.G. (1964) and A.H. (1973) submitted to the Graduate Faculty of Iowa State University, Ames, Iowa. By acceptance of this article, the publisher and/or recipient acknowledges the U.S. Government's right to retain a non-exclusive, royalty-free license in and to any copyright covering this paper.